Principles and techniques in Calorimetry

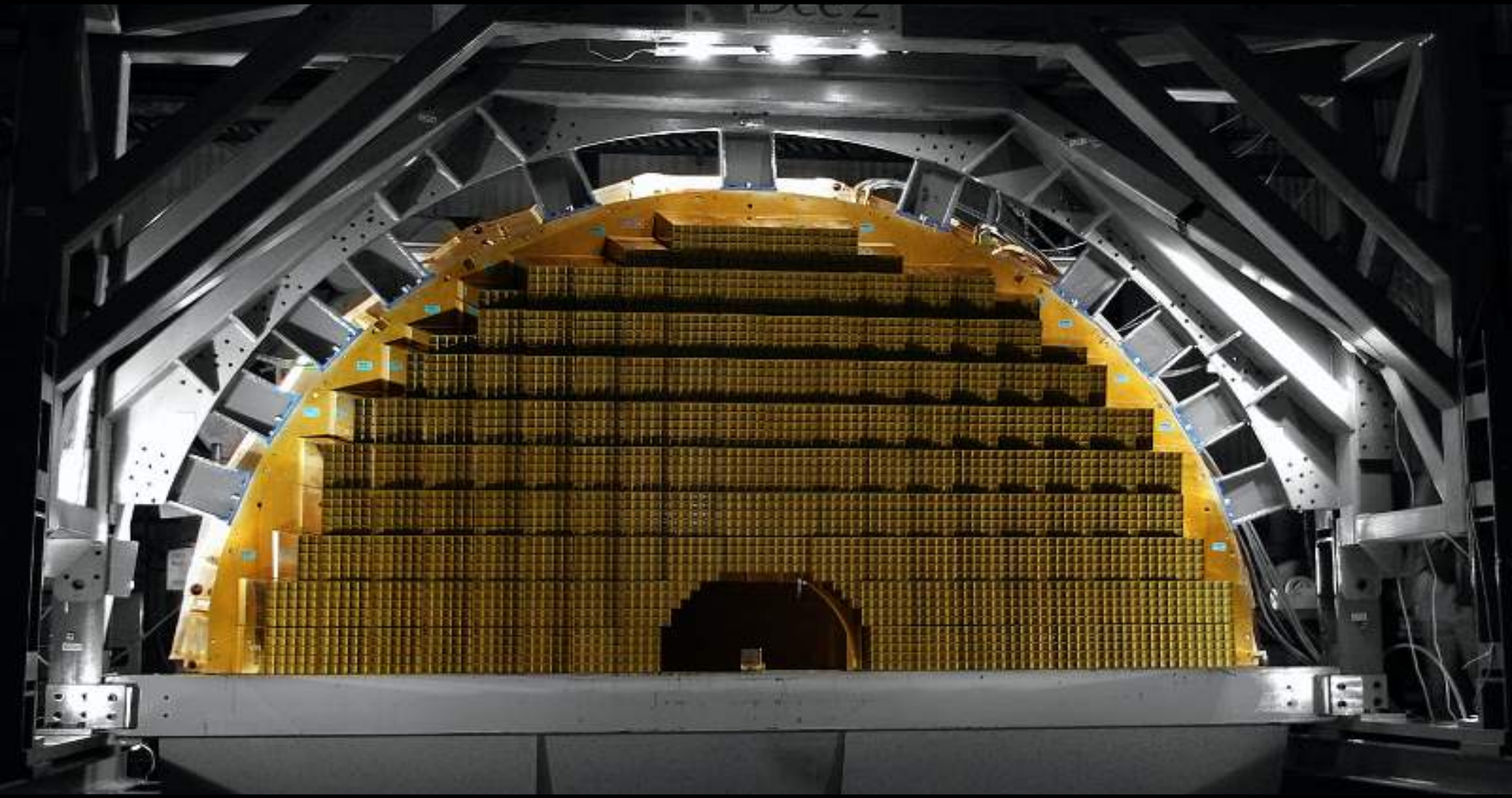

David Cockerill EIRO 11 May 2009

Overview

- Introduction
- Electromagnetic cascades
- Hadronic cascades
- Electromagnetic and Hadronic energy resolution
- Measuring jets
- Techniques for electromagnetic and hadronic calorimeters

Introduction

Calorimetry is one of the most important and powerful detector techniques in experimental particle physics

The detectors fall into two main categories

Electromagnetic calorimeters for the detection of
$e^{\pm}$, γs

Hadron calorimeters for the detection of
$\pi^{\pm}$, $p^{\pm}$, $K^{\pm}$ n, K^0_L

$\mu^{\pm}$ usually traverse the calorimeters, losing small amounts of energy by ionisation
Neutrinos are undetected, their only signature being 'Missing energy' in the detector

The 13 particles above completely dominate the types of particles from high energy collisions likely to reach and interact with the calorimeters

All other particles decay ~instantly, or in flight, usually within a few hundred microns from the collision, into one or more of the particles above

Introduction

There are two general types of calorimeter design:

Sampling calorimeters:

Layers of passive absorber (such as Pb, or Cu) alternate with active detector layers such as Si, scintillator or liquid argon → only part of the energy is sampled. Used both for electromagnetic and hadron calorimetry

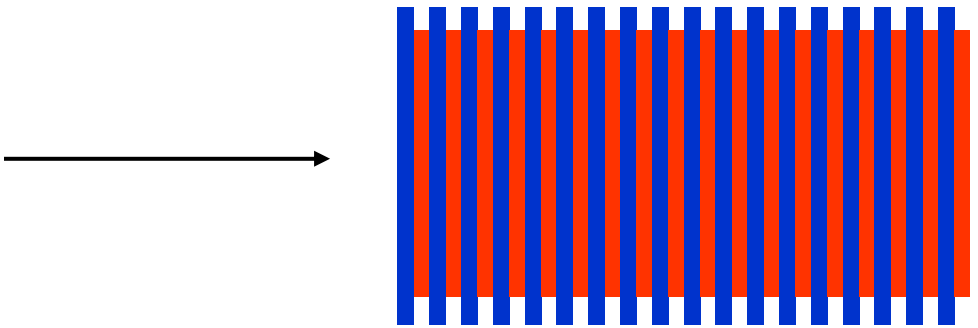

Homogeneous calorimeters:

A single medium serves as both absorber and detector, eg: liquified Xe or Kr, dense crystal scintillators (BGO, $PbWO_4$ .....), lead loaded glass.

Almost entirely for electromagnetic calorimetry

Calorimetry

- Energy measurement by total absorption, combined with spatial information
- Convert energy E of the incident particle into a detector response S
  Detector response;E

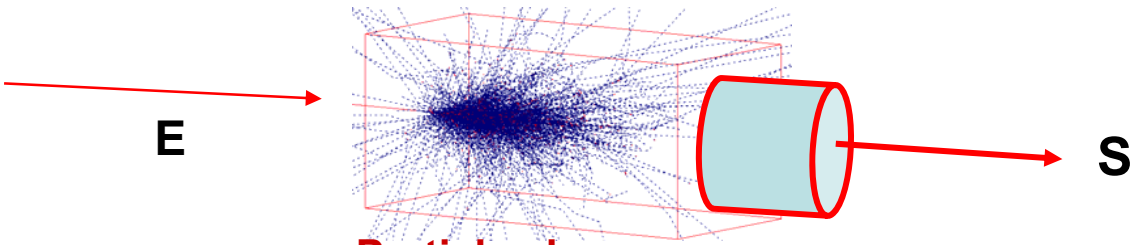

- Basic mechanism: formation of electromagnetic or hadronic showers
- Detection of both charged ($e^{\pm}$, hadrons) and neutral particles (n, γ)
- Particle identification from location of deposited energy

Calorimeters are designed to stop and fully contain their respective particles. It is the 'end of the road' for the incoming particle. Its energy is converted into ionisation or excitation of the matter

Typical configuration of calorimeters in an experiment

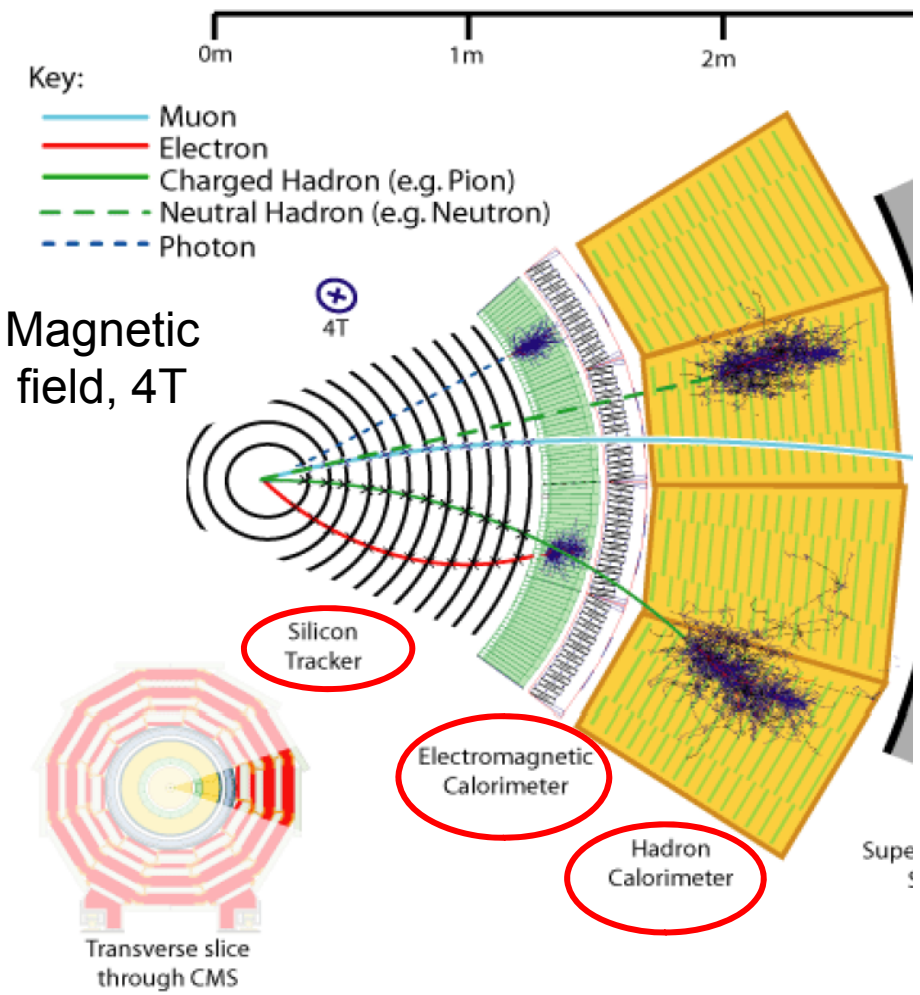

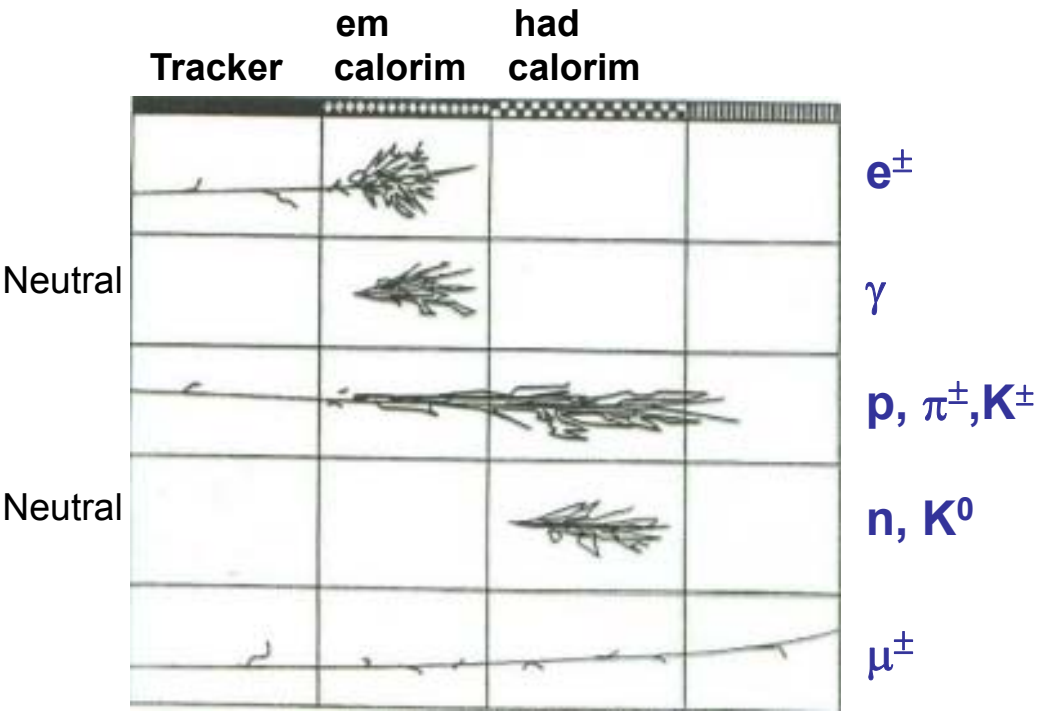

Particle identification with calorimetry using the locations of deposited energy in the calorimeters

Sign of particle charge from the Tracker

Tracker to be of minimum material to avoid losing particle energy before the calorimeters

Example – the CMS experiment at LHC

Electromagnetic calorimetry

Electromagnetic showers

- e± bremsstrahlung and photon pair production are by far the most important processes involving energy loss, especially for shower particles with energies above 1 GeV. These generate the e.m. cascade of particles in the shower.

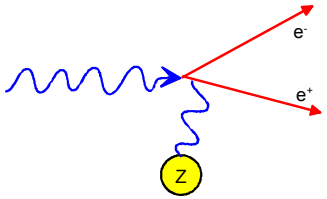

- Shower characterised by a 'radiation length', X_o, in the absorbing medium for an e± bremsstrahlung to occur

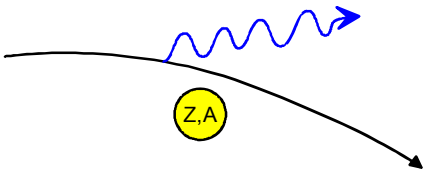

$$-\frac{dE}{dx} = 4\alpha N_A \frac{Z^2}{A} r_e^{\,2} E \ln\frac{183}{Z^{1/3}} \quad \Longrightarrow \quad -\frac{dE}{dx} \propto \frac{Z^2 E}{m^2}$$

Favours use of high Z materials for a compact calorimeter

$$-\frac{dE}{dx} = \frac{E}{X_0}$$

$$X_0 = \frac{A}{4\alpha N_A Z^2 r_e^{\,2} \ln\frac{183}{Z^{1/3}}}$$

$X_0 \sim 180\ A/Z^2$ [g cm^{-2}]

$$E = E_0\, e^{-x/X_0} \quad \Longrightarrow$$

Across 1 X_0, an e- or e+ will lose, on average, 63.2% of its energy by bremsstrahlung. In Pb (Z=82), $X_0 \sim 5.6$mm

Due to the $1/m^2$ dependence for bremsstrahlung to occur, muons only emit significant bremsstrahlung above ~1 TeV ($m_\mu \sim 210\ m_e$)

Electromagnetic showers

Pair production

Characteristic mean free path before pair production, $\lambda_{pair} = 9/7\ X_o$

$$E_\gamma \geq 2m_e c^2$$

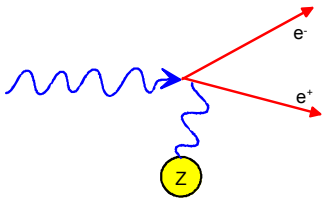

Intensity of a photon beam entering calorimeter reduced to 1/e of the original intensity, $I = I_o \exp(-7/9\ x/X_o)$. λ_{pair} = 7.2mm in Pb

Brem and pair production dominate the processes that degrade the incoming particle energy

- A 50 GeV electron
  Loses 32 GeV over 1 X_0 by bremsstrahlung

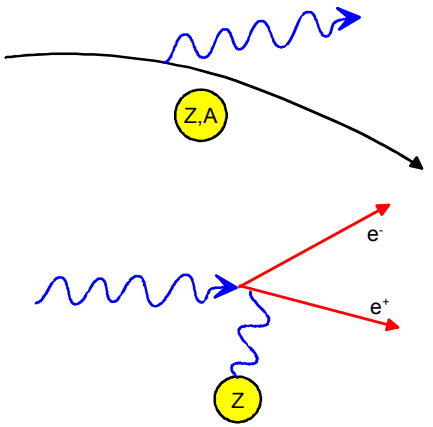

- A 50 GeV photon
  Pair production to e+ e- , 25 GeV each
  Energy regime degraded by 25 GeV

- A minimum ionising particle (m.i.p)
  In Pb, over 1 X_0, ionization loss ~O(10s) of MeV
  a factor of ~1000 less than the above

Electromagnetic showers

Below a certain energy, E_c, $e^{\pm}$ energy losses are greater through ionisation than bremsstrahlung and the multiplication process runs out

A slow decrease in number of particles in the shower occurs. Electrons/positrons are stopped

Photons progressivley lose energy by compton scattering, converting to electrons via the photo-electric effect, and absorption

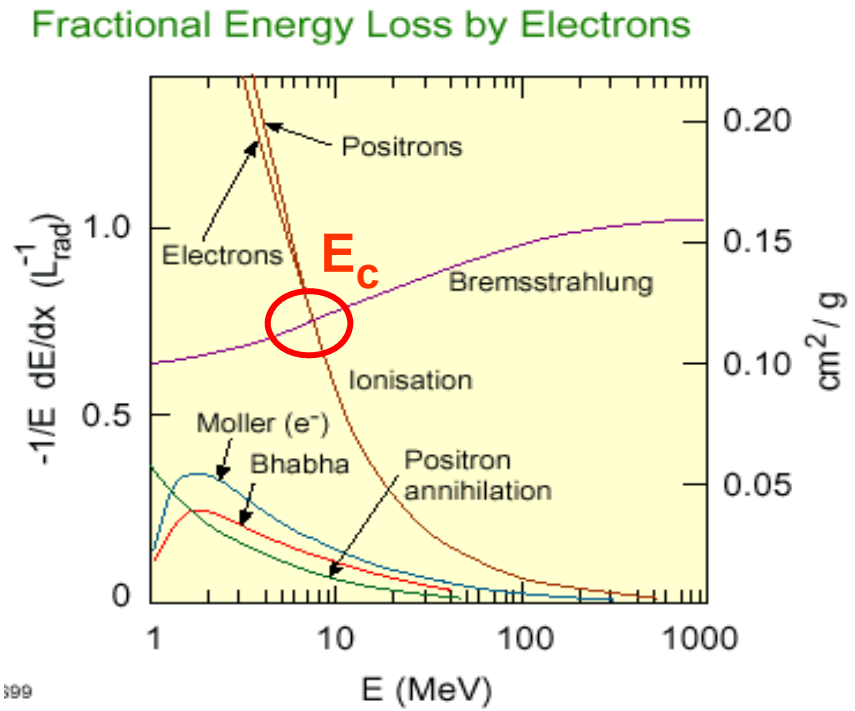

$$E_c \approx \frac{610MeV}{Z+1.24}$$

Liquids and solids

For Pb (Z=82), E_c = 7.3 MeV
For Cu (Z=29), E_c = 20.2 MeV

The higher coulomb field in Pb means that bremstrahlung dominates over ionisation to much lower shower particle energies than in Cu

As a consequence, the shower depth, in Xo, is slightly deeper in Pb than in Cu.

EM showers: a simple model

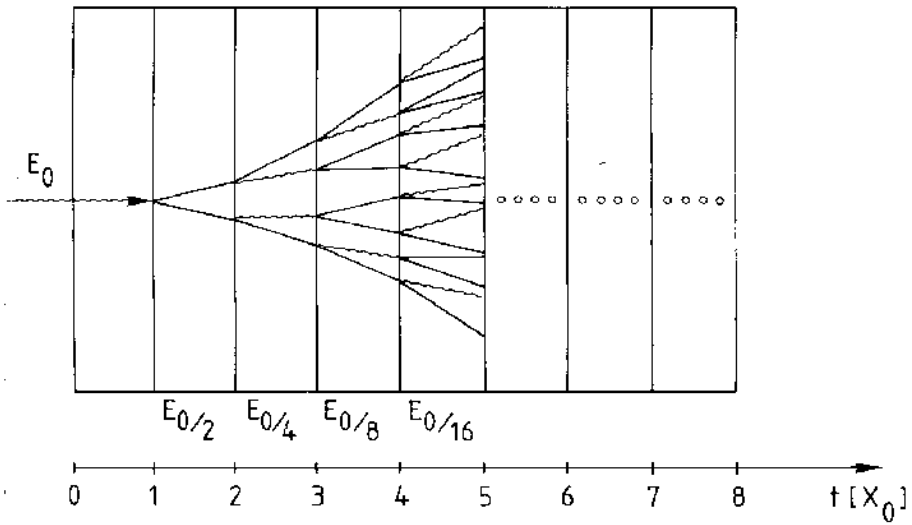

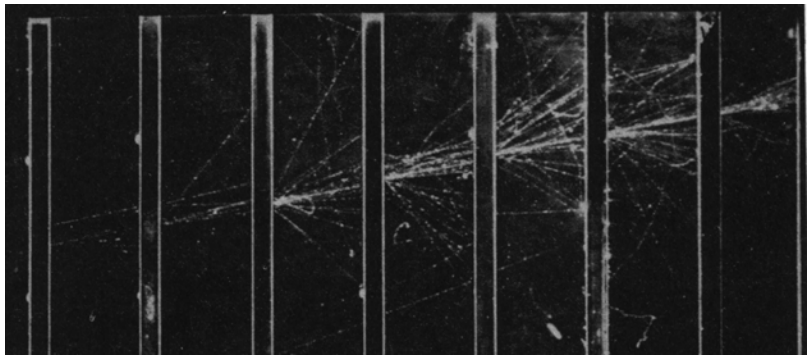

Electron shower in a cloud chamber with lead absorbers

Consider only Bremstrahlung and pair production

Assume $X_0 = \lambda_{pair}$

Assume, in each generation, number of particles increases by factor 2

$$N(t) = 2^t \qquad E(t)/particle = E_0 \cdot 2^{-t}$$

Process continues until $E(t) < E_c$

$$t_{\max} = \frac{\ln E_0/E_c}{\ln 2}$$

$$N^{total} = \sum_{t=0}^{t_{\max}} 2^t = 2^{(t_{\max}+1)} - 1 \approx 2 \cdot 2^{t_{\max}} = 2\frac{E_0}{E_c}$$

50 GeV e- on lead

N^{total} ~ 14000 particles, t_{max}~13 X_o (over estimate)

EM showers profiles

Longitudinal shower development

Shower maximum at $t_{max} \sim \ln(E_o/E_c) - 0.5$ for $e^{\pm}$
$t_{max} \sim \ln(E_o/E_c) + 0.5$ for γ

95% containment $t_{95\%} \approx t_{\max} + 0.08Z + 9.6$

Size of a calorimeter grows only logarithmically with E_o

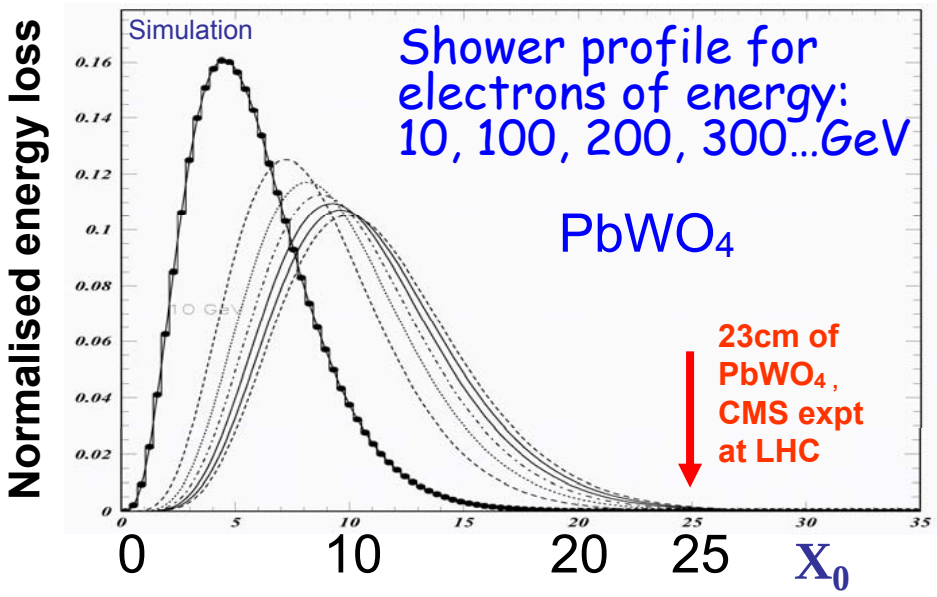

Transverse shower development

Multiple Coulomb scattering by $e^{\pm}$ in shower.

95% of the shower cone is located in a cylinder with radius 2 R_M

$$R_M = \frac{21\,\text{MeV}}{E_c} X_0 \quad [g/cm^2]$$ Molière radius

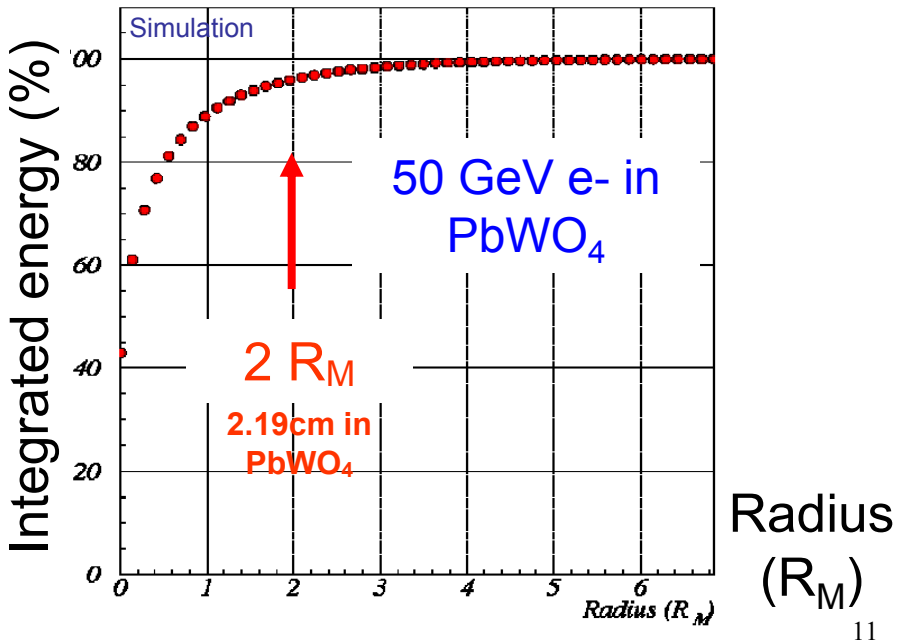

Example 100 GeV e- in lead glass, $X_o \sim 2$cm
$t_{95\%} \sim 23\ X_o$ = 46cm
$R_M \sim 1.8\ X_o$ = 3.6 cm

EM showers profiles

EM shower development in krypton (Z=36, A=84)

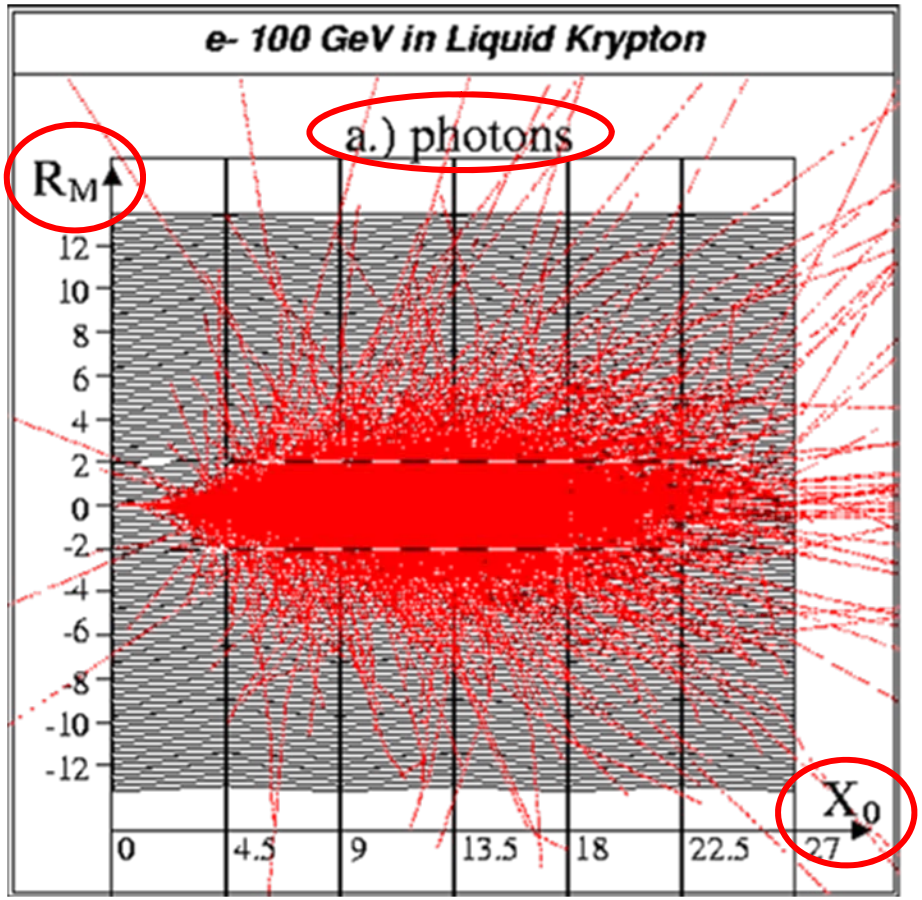

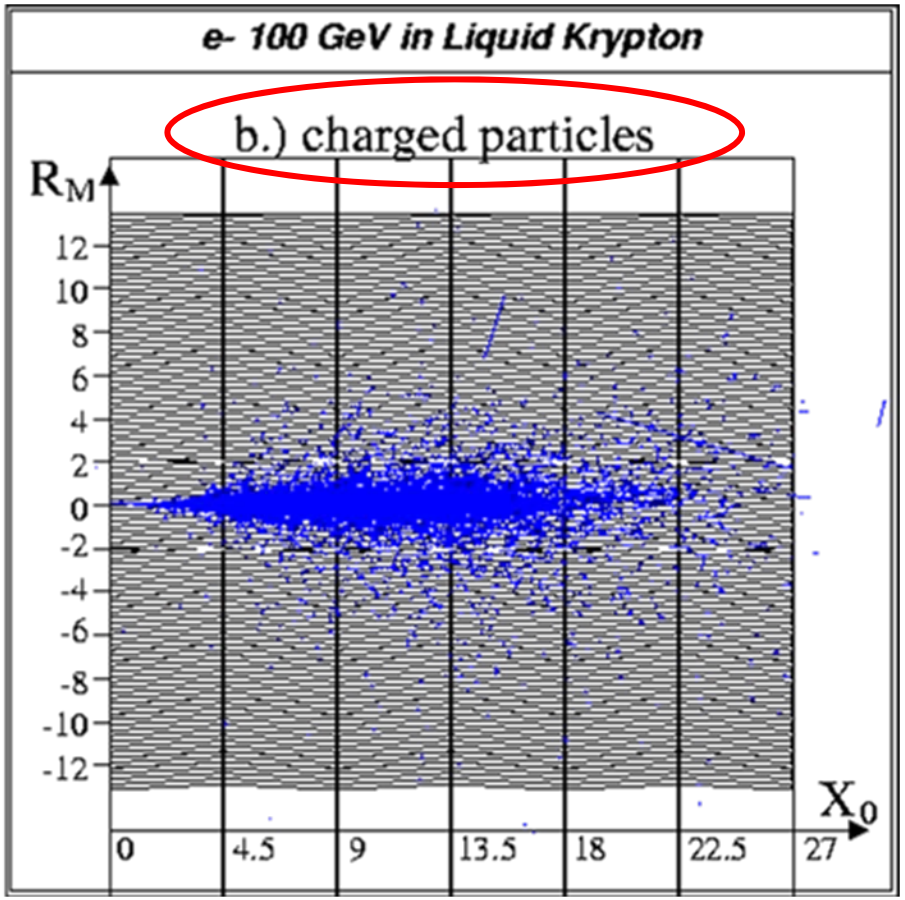

GEANT simulation of a 100 GeV electron shower in the NA48 liquid Krypton calorimeter

Hadronic Calorimetry

Hadronic cascades Much more complex than e.m. cascades

Shower development determined by the mean free path, λ_I, between inelastic collisions

The nuclear interaction length is given by $\lambda_I = A / (N_A.\sigma_{inel})$, $\sigma_{inel} \approx \sigma_0 A^{0.7}$ $\sigma_0 \approx 35\ mb$

Simple model, expect $\sigma_I \propto A^{2/3}$ and thus $\lambda_I \propto A^{1/3}$. In practice $\lambda_I \sim 35\ A^{1/3}$

High energy hadrons interact with nuclei producing secondary particles, mostly $\pi\pm$ and π^o

Lateral spread of shower from transverse energy of secondaries, $\langle p_T \rangle \sim 350$ MeV/c

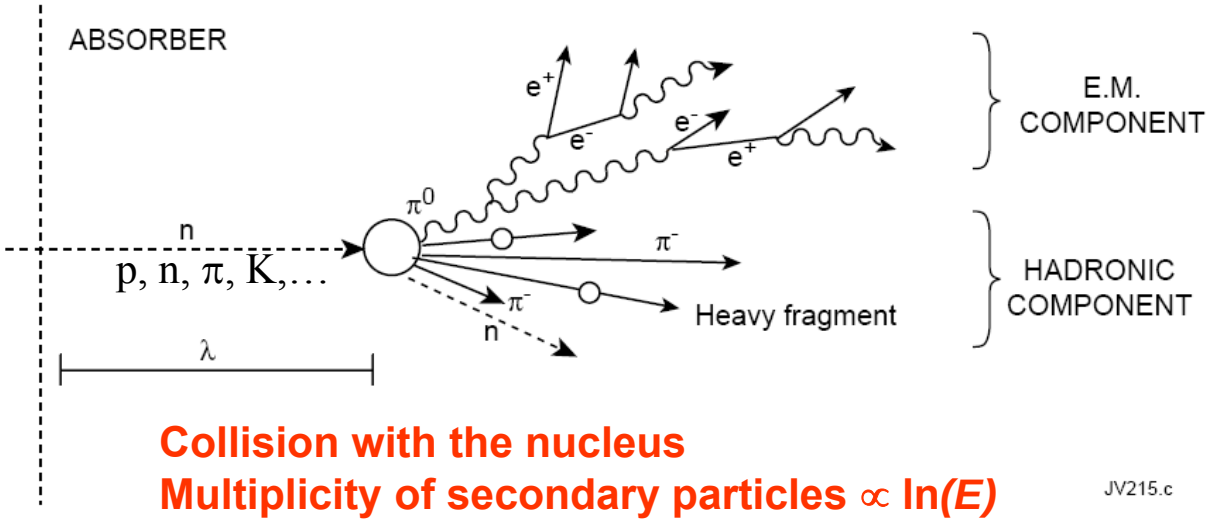

Collision with the nucleus
Multiplicity of secondary particles $\propto$ ln*(E)*
$n(\pi^0) \sim \ln E\ (GeV) - 4.6$
For a 100 GeV incoming hadron, $n(\pi^0) \approx 18$

~ 1/3 of the pions produced are π^0 which decay $\pi^0 \rightarrow \gamma\gamma$ in $\sim 10^{-16}$s

Thus the cascades have two distinct components: hadronic and electromagnetic

Hadronic Calorimetry

Simulations of hadron showers

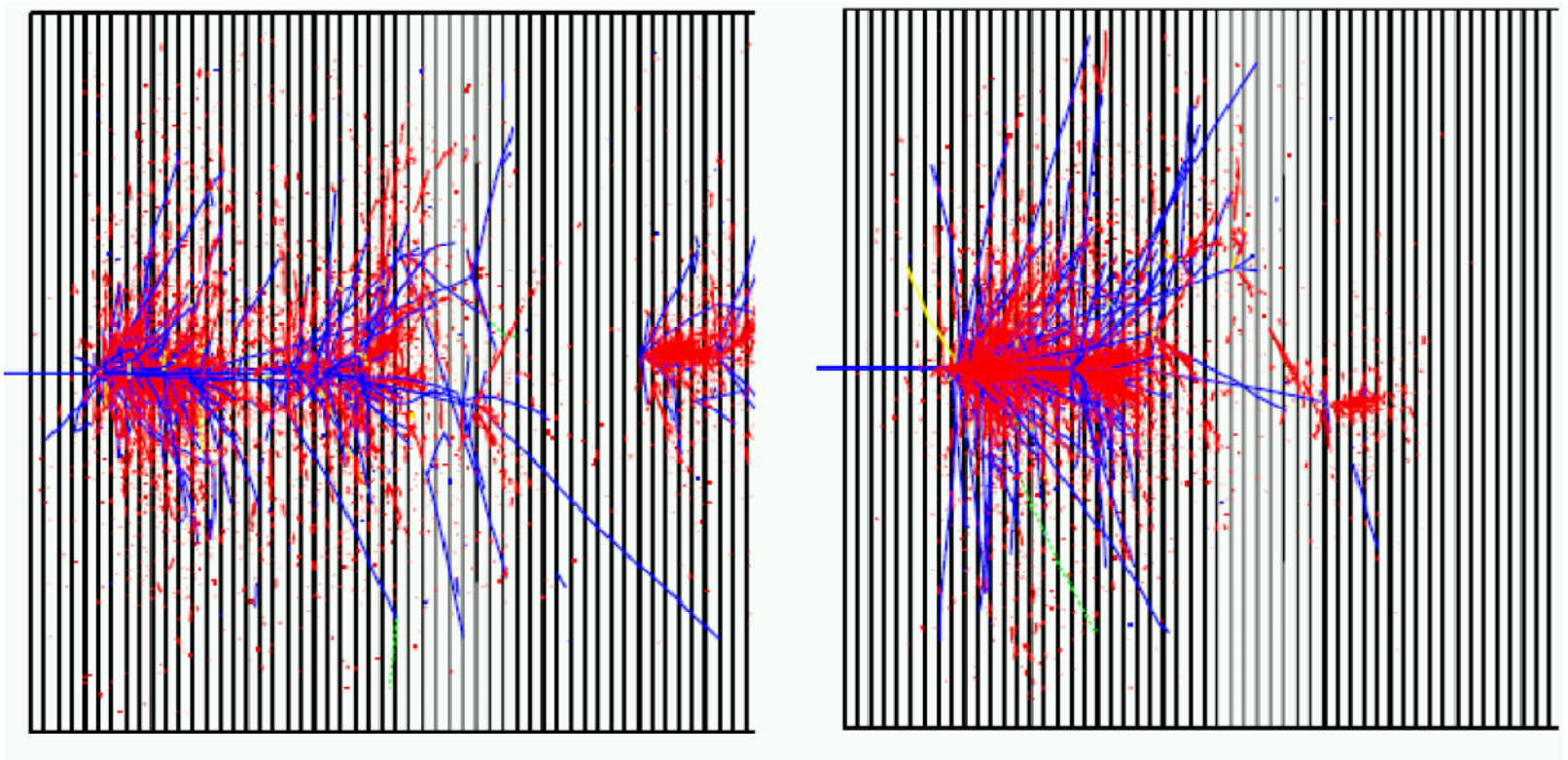

Red - e.m. component Blue – charged hadrons

Unlike electromagnetic showers, hadron showers do not show a uniform deposition of energy throughout the detector medium

Hadronic Calorimetry

Hadronic longitudinal shower development

$$t_{\max}(\lambda_I) \approx 0.2 \ln E[GeV] + 0.7$$

$$t_{95\%}(cm) \approx a \ln E + b$$

For Iron: a = 9.4, b=39 λ_I=16.7 cm

E =100 GeV → $t_{95\%} \approx$ 80 cm of iron

Hadronic lateral shower development

The shower consists of core + halo

95% containment in a cylinder of radius λ_I

Hadronic showers are much longer and broader than electromagnetic ones !

In dense materials

$X_0 \sim 180\ A / Z^2 \ll \lambda_I \sim 35\ A^{1/3}$

e.g. Iron X_0 = 1.8 cm ⇔ λ_I = 16.7 cm

The e.m. component develops more rapidly than the hadronic. The shower profile is characterised by a peak close to the first interaction, followed by an exponential fall off with scale λ_I

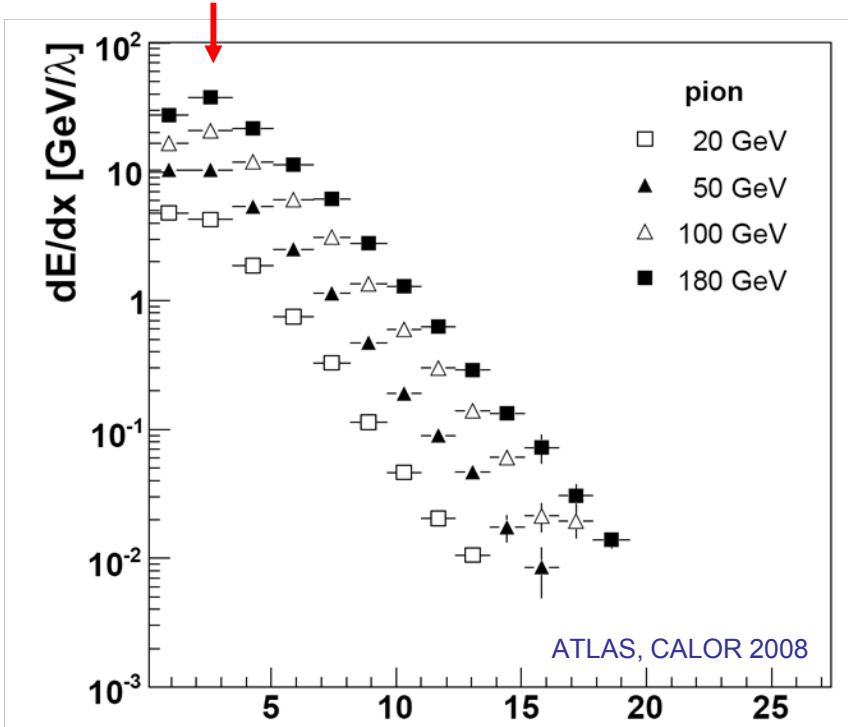

Longitudinal profile of pion induced showers at various energies

Substantial difference between em and hadronic shower size → hadron calorimeters much larger than em calorimeters

Energy resolution

Energy resolution of a calorimeter often parameterised as

$$\frac{\sigma}{E} = \frac{a}{\sqrt{E}} \oplus \frac{b}{E} \oplus c$$

Relative energy resolution of a calorimeter improves with E_0
Also spatial and angular resolution scale like $1/\sqrt{E}$

a , stochastic term arising from fluctuations in the number of signal generating processes, ie on the number of photo-electrons generated

b , noise term includes noise in readout electronics, and 'pile-up' due to other collision events generating pcles which arrive close in time

c , constant term imperfections in calorimeter construction (dimension variations)
non-uniform detector response
channel to channel intercalibration errors
fluctuations in longitudinal energy containment
energy lost in dead material, before or in detector

For e.m calorimetry, energy resolution at high energy usually dominated by c

Goal of calorimeter design - find best compromise between these three contributions

Intrinsic Energy Resolution

Intrinsic resolution of homogeneous e.m. calorimeters

Principle of e.m. calorimetry – that energy released in the detector material (mainly ionisation, excitation) is proportional to the energy of incident particle

If Q is the mean energy required to produce a 'visible' photon in a crystal, or an electron-ion pair in a noble liquid, then the mean number of quanta produced is

$$\langle n \rangle = E_0 / Q$$

The intrinsic energy resolution is given by the fluctuations on n

At first sight $\sigma_E / E = \sqrt{n} / n = \sqrt{(Q / E)}$ and typically $\sigma_E/E \sim (1 \div 3)\%/\sqrt{E}$

However, in certain cases, the energy of the incident particle is only transferred to making quanta, and to no other energy dissipating processes. Fluctuations are much reduced. Instead $\sigma_E / E = \sqrt{(FQ / E)}$ where F is the 'Fano' factor

Intrinsic resolution of sampling e.m. calorimeters

Sampling fluctuations arise due to variations in the number of charged particles crossing the active layers $n_{ch} \propto Eo / t$ (t = thickness of each absorber layer)

If each sampling is independent then $\sigma_{samp} / E = 1/\sqrt{n_{ch}} \propto \sqrt{(t / E)}$
Need ~100 sampling layers to compete with homogeneous devices. Typically $\sigma_{samp}/E \sim 10\%/\sqrt{E}$

Resolution of crystal em calorimeters

Widely used class of homogeneous em calorimeter employs large, dense, monocrystals of inorganic scintillator. E.g the CMS crystal calorimeter which uses PbWO4 crystals

Scintillation emission only small fraction of energy loss in xtal, so *F ~ 1*

However - fluctuations in the avalanche process in the Avalanche Photodiodes used for the photodection gives rise to an excess noise factor in the gain of the device

This leads to *F ~ 2* for the xtal + APD combination

PbWO4 – a relativley weak scintillator
~ 4500 photo-electrons released by APD for 1 GeV of deposited energy

Thus, coefficient of stochastic term

$$a_{pe} = \sqrt{F / Npe} = \sqrt{(2 / 4500)} = 2.1\%$$

However this assumes perfect shower containment. In practice energy summed over limited 3x3, or 5x5, clusters of xtals (to minimise added noise)

Expect $a_{leak} = 2\%$ from an energy sum over a 3x3 array of crystals

Thus expect $a = a_{pe} \oplus a_{leak} = 2.9\%$
Measured value $= 2.8\%$

Resolution of hadronic calorimeters

Absorber depth required to contain hadron showers ~ 10 λ_I = 135cm of Cu

Hadron calorimeters almost all sampling calorimeters

Several processes contribute to hadron energy dissipation, eg in Pb:

Nuclear break-up (invisible) 42%
Charged particle ionisation 43%
Neutrons with T_N ~ 1 MeV 12%
Photons with E_γ ~ 1 MeV 3%

In general, hadronic component of hadron shower produces smaller signal than the em component so $e/h > 1$
F_{π^0} ~ *1/3* at low energies, increasing with energy
$F\pi^\circ \sim a \log(E)$
(since em component 'freezes out')

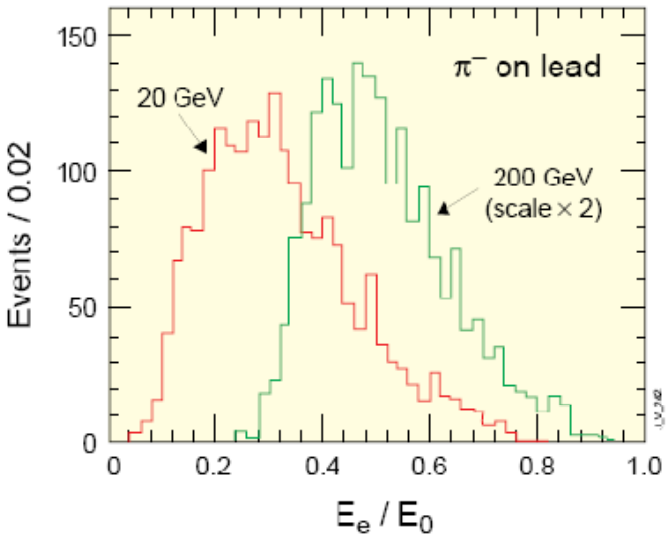

If $e/h \neq 1$:- response with energy is non-linear
- fluctuations on F_{π° contribute to σ_E/E

Furthermore, since the fluctuations are non-Gaussian, σ_E/E scales more weakly than $1/\sqrt{E}$

Constant term: Deviations from $e/h = 1$ also contribute to the constant term.

In addition calorimeter imperfections contribute: inter-calibration errors, response non-uniformity (both laterally and in depth), energy leakage and cracks .

Jet energy resolution

At colliders, hadron calorimeters serve primarily to measure jets and missing ET:
For a single particle: $\sigma_E / E = a / \sqrt{E} \oplus c$ (neglect electronic noise)

At low particle energy, resolution is dominated by a,
at high energy by c

If the stochastic term, a, dominates:
- error on Jet energy same as for
  a single particle of the same energy

If the constant term dominates:
- error on Jet energy is less than for
  a single particle of the same energy

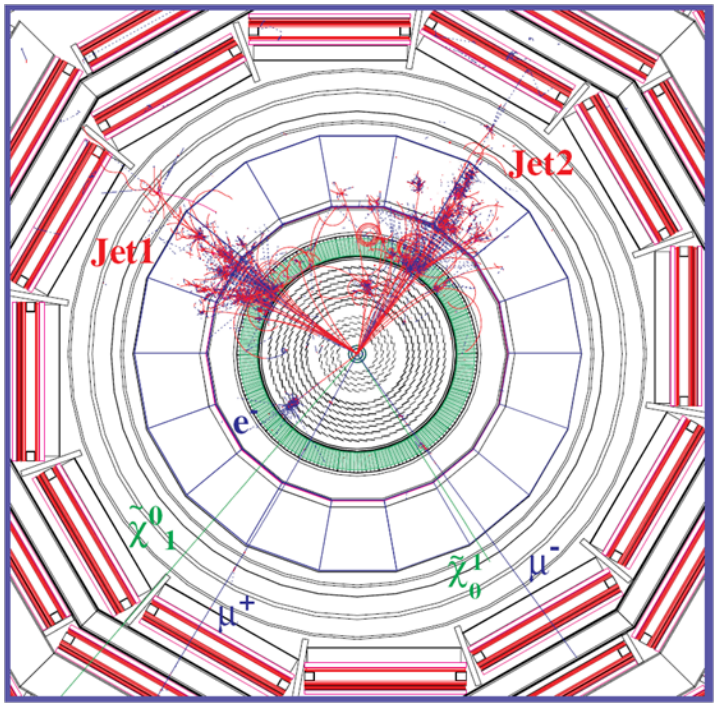

Jets from a simulated event in CMS

For a calorimeter with $\sigma_E / E = 0.3 / \sqrt{E} \oplus 0.05$
1 TeV jet composed of four hadrons of equal energy has $\delta E_{Jet} = 25$ GeV,
compared to $\delta E = 50$ GeV, for a single 1 TeV hadron

Jet measurements in the future - particle flow calorimetry ?

Traditional approach – all components of jet energy measured in ECAL/HCAL

In a typical jet 60% jet energy charged hadrons
30% in photons (mainly from π -> $\gamma\gamma$)
10% in neutral hadrons

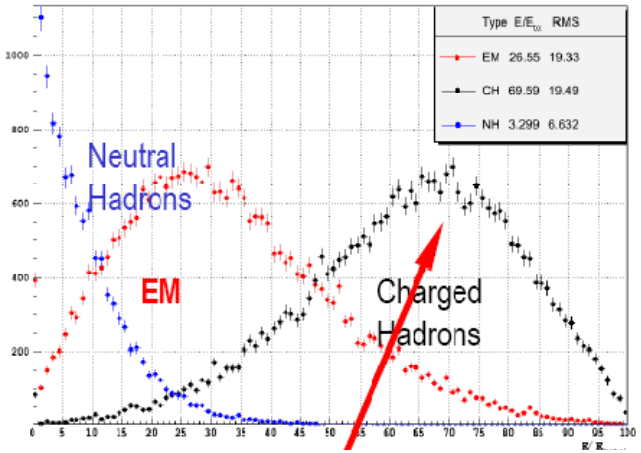

Measure these in the tracker

Particle flow paradigm to better measure jets ?
- Charged particles measured in tracker
- Photons in ECAL
- Neutral hadrons in HCAL (+ECAL)
- Only 10% of jet energy measured in 'poor' HCAL

But - need to separate energy deposits from different pcles

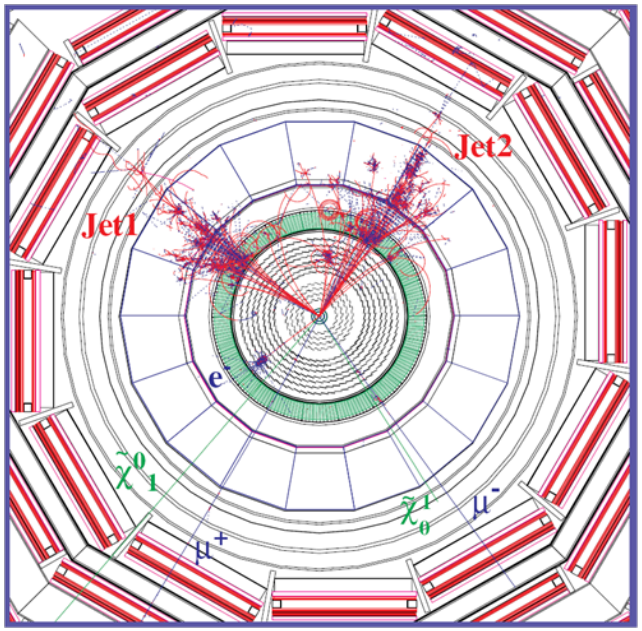

Need - very high transverse segmentation
ECAL ~1x1 cm^2 SiW project – CALICE
HCAL ~3x3 cm^2 Steel/scintillator
And high longitudinal sampling, 30 layers ECAL, 40 HCAL

Opportunities for tomorrow's technologists !

Homogeneous calorimeters

Lead glass, SF-6, X_o = 1.69cm, ρ = 5.2 g/cm^3

Three main types: scintillating crystals, Glass blocks (Cerenkov radiation), Noble liquids

Crystals	NaI(Tl)	CsI(Tl)	CsI	BGO	$PbWO_4$
Density (g/cm^3)	3.67	4.53	4.53	7.13	8.28
X_0 (cm)	2.59	1.85	1.85	1.12	0.89
R_M (cm)	4.5	3.8	3.8	2.4	2.2
Decay time (ns)	250	1000	10	300	5
slow component			36		15
Emission peak (nm)	410	565	305	410	440
slow component			480		
Light yield γ/MeV	4×10^4	5×10^4	4×10^4	8×10^3	1.5×10^2
Photoelectron yield (relative to NaI)	1	0.4	0.1	0.15	0.01
Rad. hardness (Gy)	1	10	10^3	1	10^5

Barbar @PEPII 10ms inter'n rate good light yield, good S/N

KTeV at Tevatron, High rate, Good resolution

L3@LEP, 25μs bunch crossing, Low rad'n dose

CMS@LHC, 25ns bunch crossing, high radiation dose

Noble liquids for homogeneous calorimeters

Lead glass, SF-6, X_o = 1.69cm, ρ = 5.2 g/cm^3

	Ar	Kr	Xe
Z	18	36	58
A	40	84	131
X_0 (cm)	14	4.7	2.8
R_M (cm)	7.2	4.7	4.2
Density (g/cm^3)	1.4	2.5	3.0
Ionization energy (eV/pair)	23.3	20.5	15.6
Critical energy ϵ (MeV)	41.7	21.5	14.5
Drift velocity at saturation (mm/μs)	10	5	3

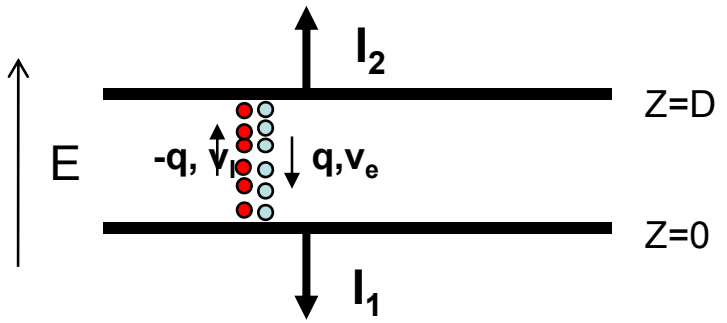

E.g. Liquid Argon, 5mm/ µs at 1kV/cm, 5mm gap → 1 µs for all electrons to reach the electrode.

The ion velocity is 10^3 to 10^5 times smaller → doesn't contribute to the signal for electronics of µs integration time.

When charged particle traverses these materials, half lost energy converted to ionisation, half to scintillation

Both rarely collected – difficult technically

Kr for most compact calorimeter
Ar for low cost, high purity

Homogeneous electromagnetic calorimeters

CMS at the LHC – scintillating $PbWO_4$ crystals

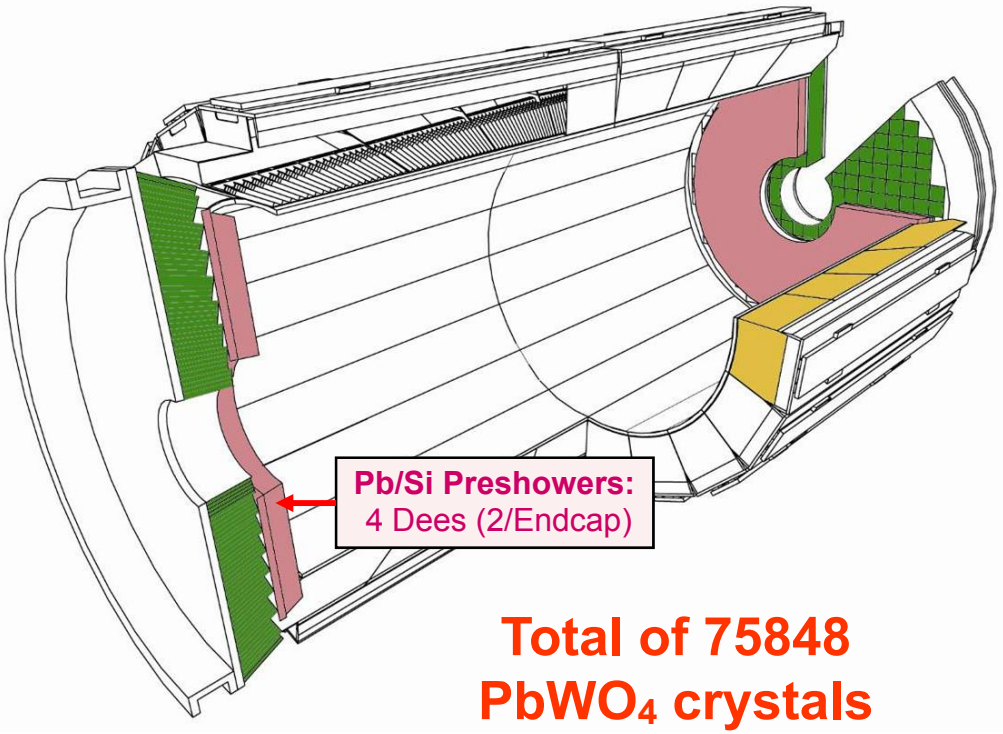

Total of 75848 $PbWO_4$ crystals

Barrel: 36 Supermodules (18 per half-barrel)
61200 Crystals (34 types) – total mass 67.4 t

Endcaps: 4 Dees (2 per Endcap)
14648 Crystals (1 type) – total mass 22.9 t

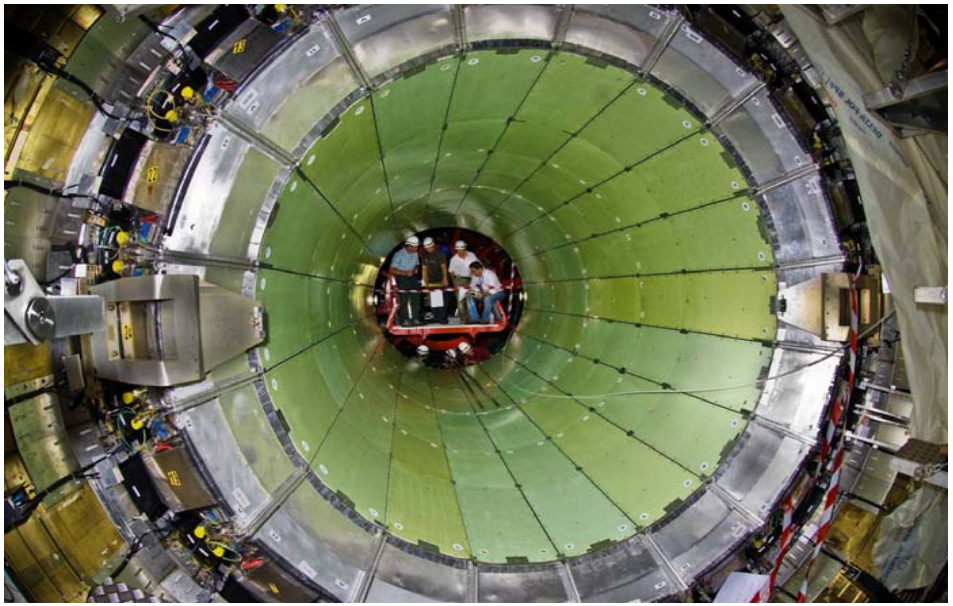

CMS Barrel

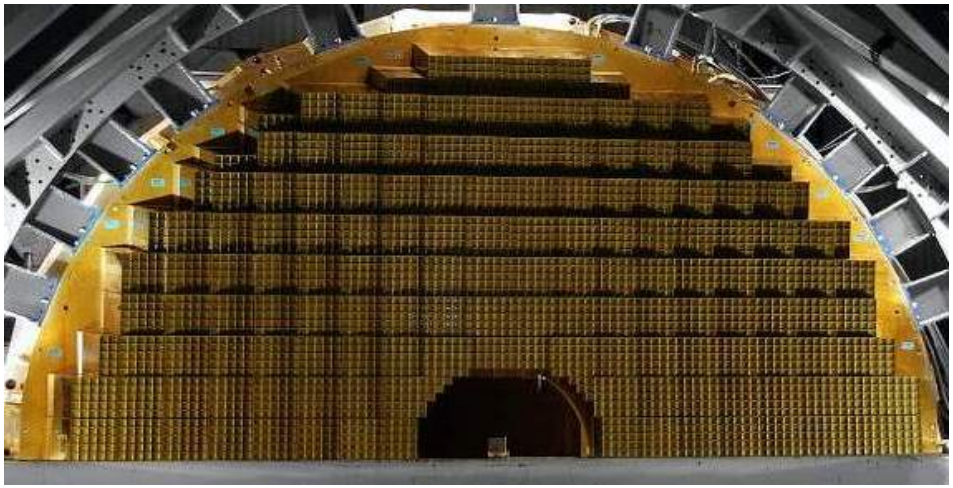

An endcap Dee, 3662 crystals awaiting transport

ALICE at the LHC – scintillating $PbWO_4$ crystals

Avalanche photo diode readout

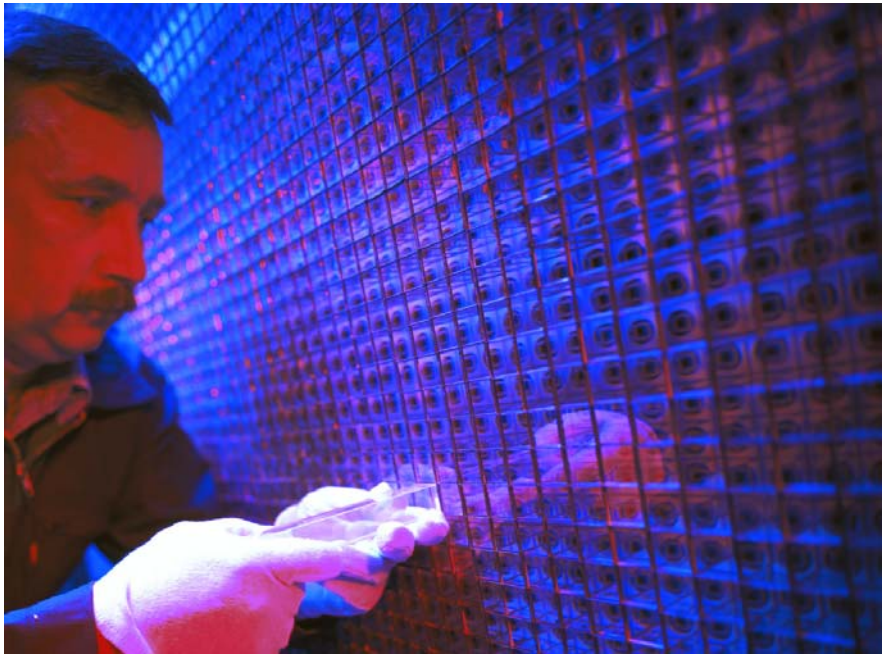

Stunning views of the array of some of the 17,920 $PbWO_4$ crystals for ALICE (PHOS)

Homogeneous calorimetry – lead tungstate crystal scintillator

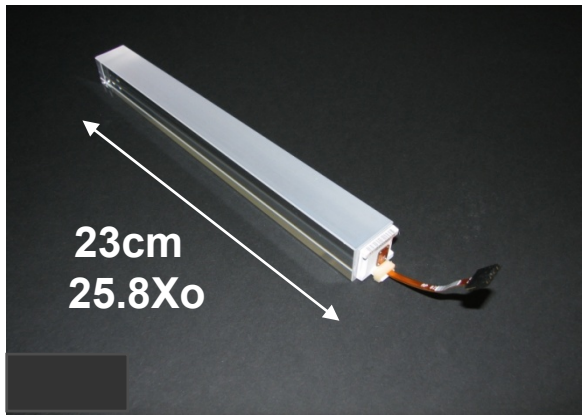

CMS Barrel crystal, tapered ~2.6x2.6 cm^2 at rear Avalanche Photo Diode readout

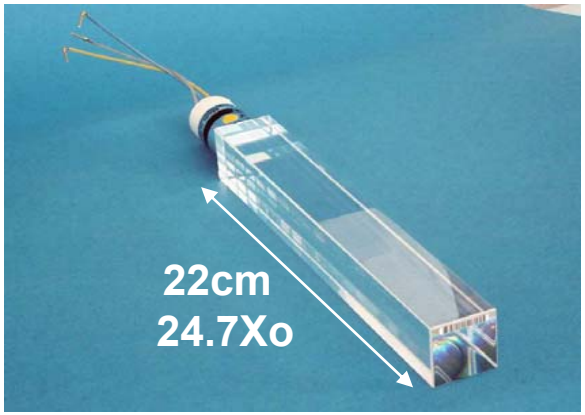

CMS Endcap crystal, tapered, 3x3 cm^2 at rear Vacuum Photo Triode readout

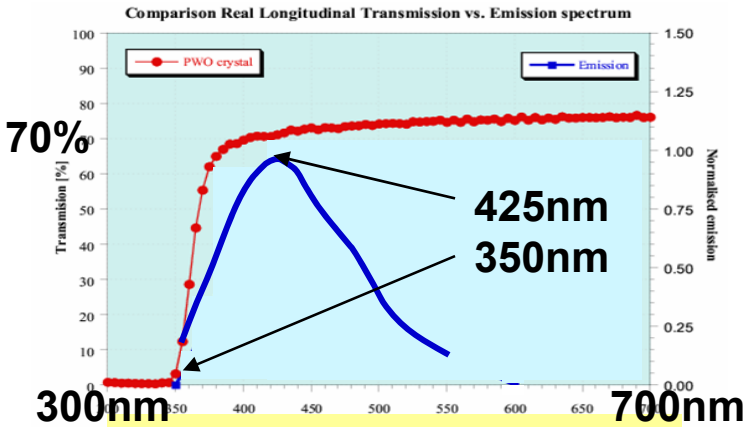

Emission spectrum (blue) and transmission curve

Reasons for $PbWO_4$

Homogeneous medium

Fast light emission	~80% in 25 ns
Short radiation length	X_0 = 0.89 cm
Small Molière radius	R_M = 2.10 cm
Emission peak	425nm

Reasonable radiation resistance to very high doses

Homogeneous calorimetry

CMS $PbWO_4$ - photodetectors

Barrel

Avalanche photodiodes(APD)

Two 5x5 mm^2 APDs/crystal

Gain 50

QE ~75%

Temperature dependence -2.4%/^{O}C

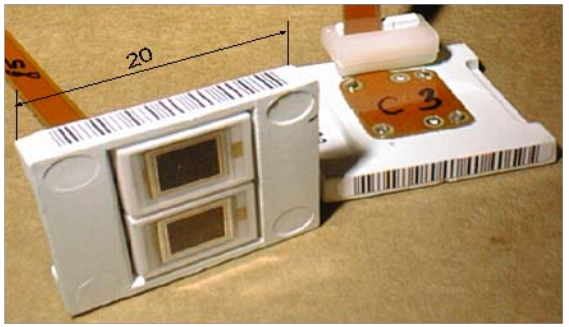

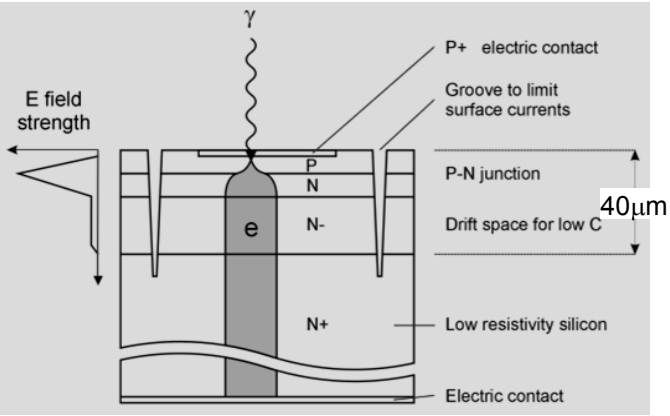

Endcaps

Vacuum phototriodes(VPT)

More radiation resistant than Si diodes

- UV glass window
- Active area ~ 280 mm^2/crystal
- Gain 8 -10 (B=4T)
- Q.E. ~20% at 420nm

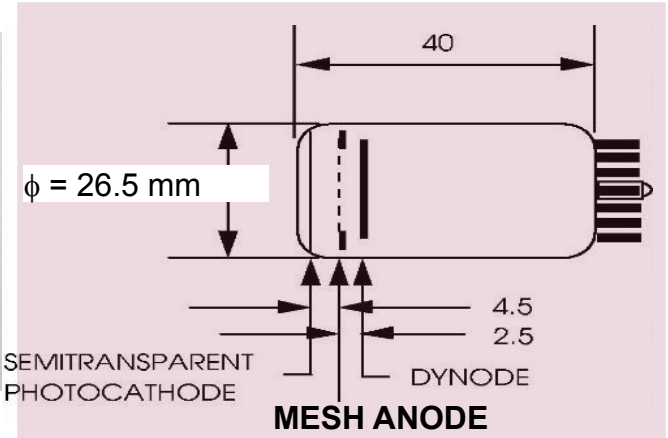

$PbWO_4$ - CMS ECAL energy resolution

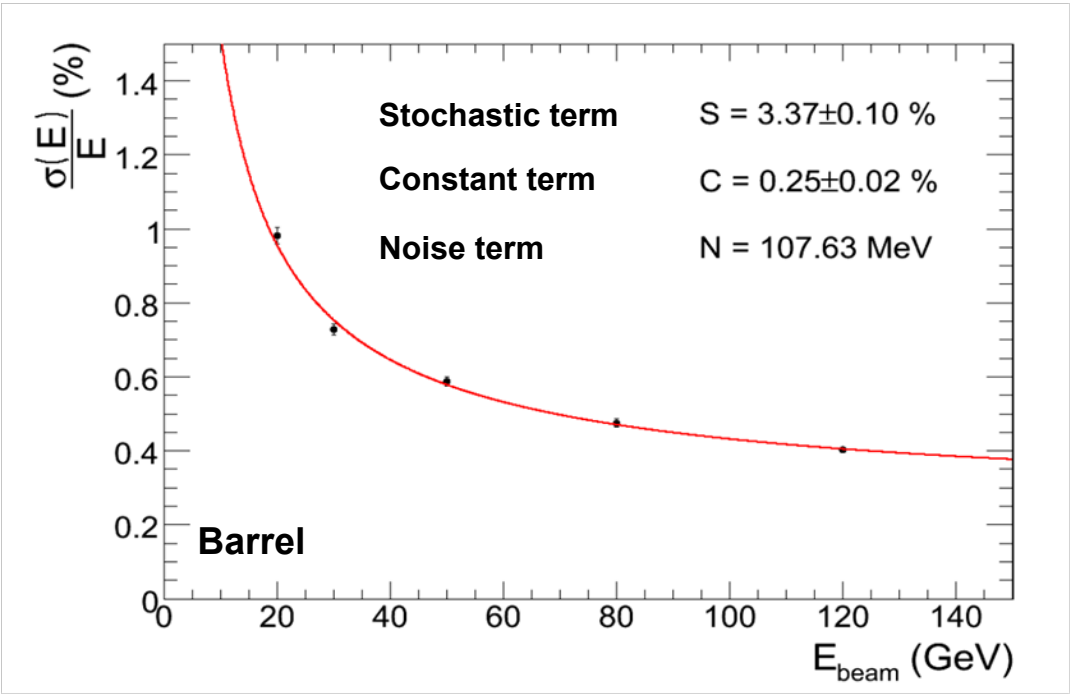

Electron energy resolution as a function of energy

Electrons centrally (4mmx4mm) incident on crystal

Resolution 0.4% at 120 GeV

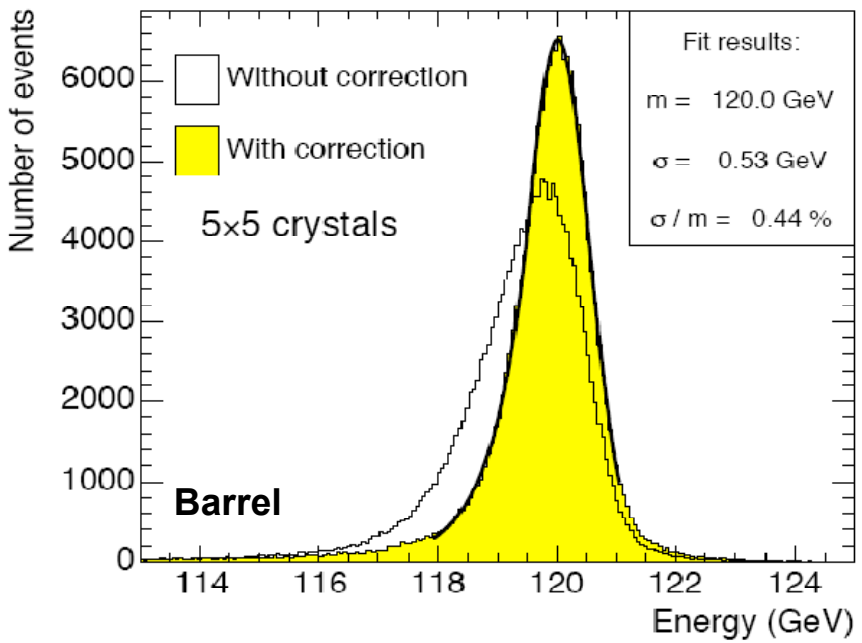

Energy resolution at 120 GeV

Electrons incident over full crystal face

Energy sum over 5x5 array wrt hit crystal.

Universal position 'correction function' for the reconstructed energy applied

Resolution 0.44%

Sampling electromagnetic calorimeters

ATLAS at the LHC – the Accordion sampling, liquid argon calorimeter

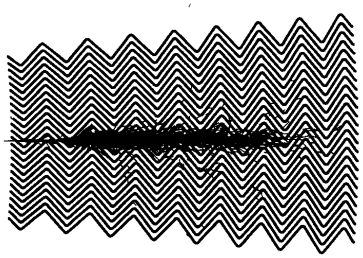

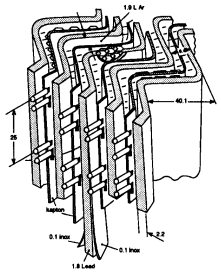

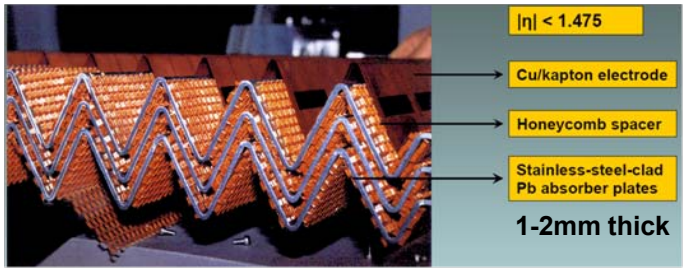

Absorbers immersed in liquid argon (90K)
Multilayer Cu-polyimide readout boards
Electric field to collect ionisation,
1 GeV energy deposit → 5.10^6 e^-

Accordion geometry minimises dead zones
Liquid argon intrinsically rad hard
Readout board allows fine segmentation
(azimuth, rapidity, longitudinal)

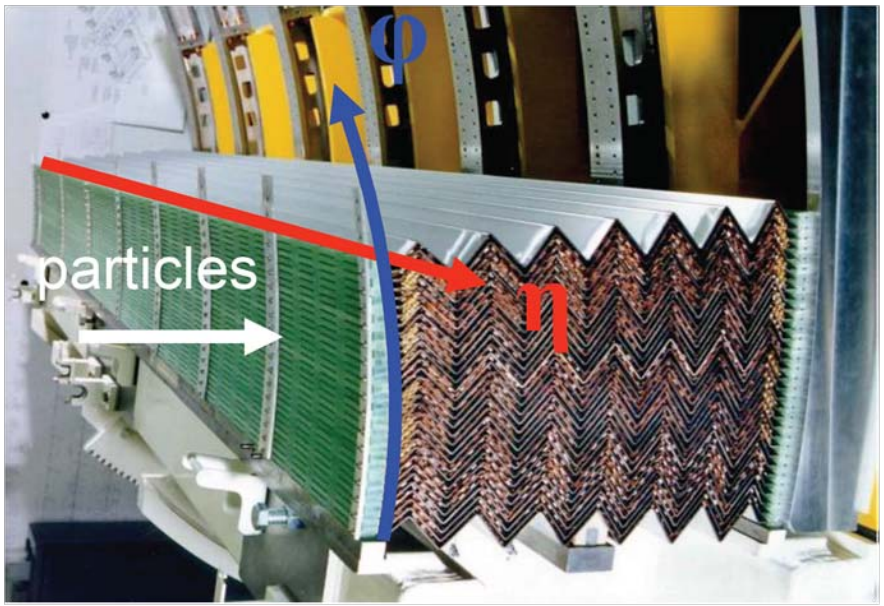

Test beam results, e^- 300 GeV (ATLAS TDR)

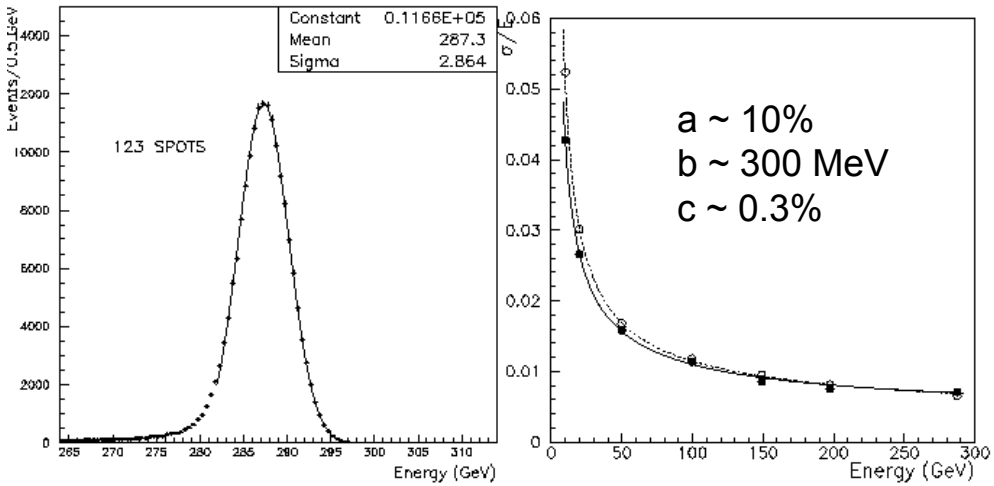

Spatial resolution ~5mm / $\sqrt{E}$ (GeV)

Sampling electromagnetic calorimeters

NA48 Liquid Krypton Ionisation chamber (T = 120K)

No metal absorbers: quasi homogeneous

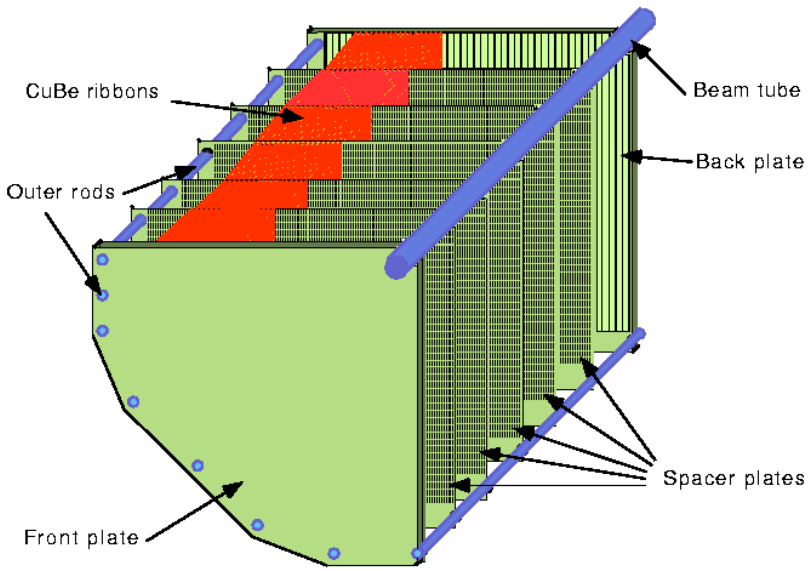

NA48 Liquid Krypton
2cmx2cm cells
X_0 = 4.7cm
125cm length (27X_0)
ρ = 5.5cm

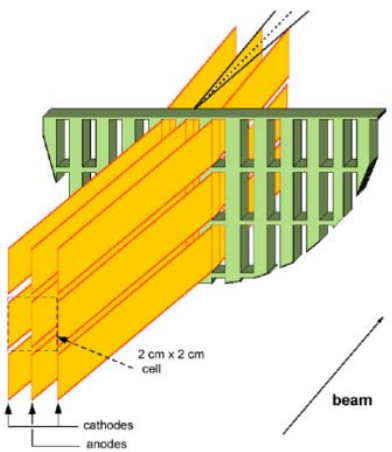

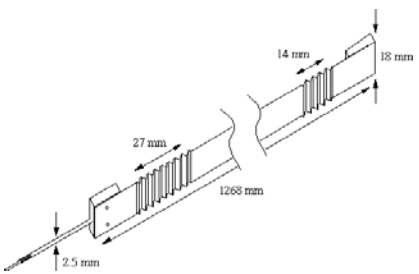

Cu-Be ribbon electrode

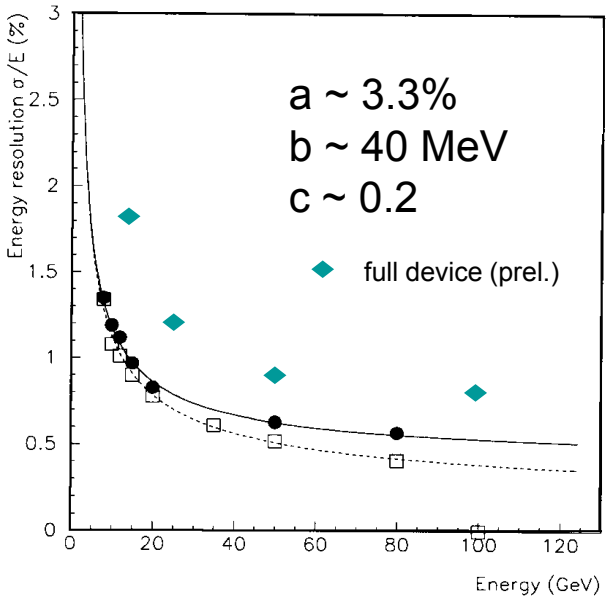

Hadron Sampling Calorimeters

CMS Hadron calorimeter

Workers in Murmansk sitting on brass casings of decommissioned shells of the Russian Northern fleet

Casings melted in St Petersburg and turned into raw brass plates

Machined in Minsk and mounted to become absorber plates for the CMS Endcap Hadron Calorimeter.

(Explosives previously removed!)

Brass absorber preparation

CMS Hadron sampling calorimetry

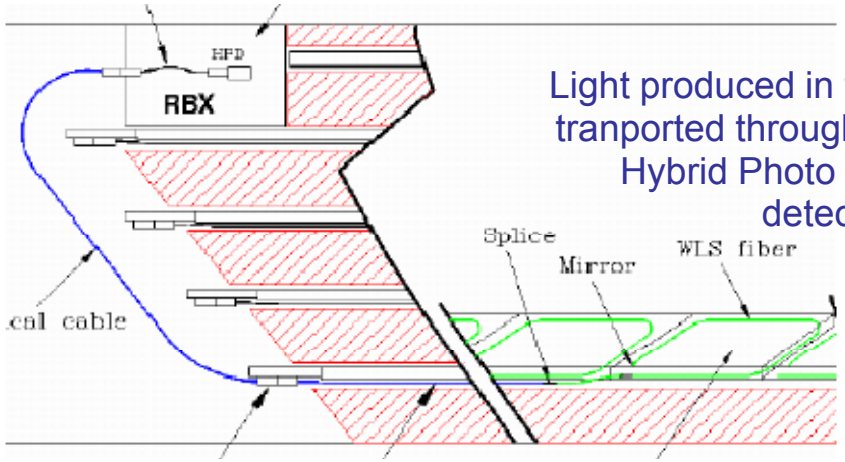

Light produced in the scintillators is tranported through optical fibres to Hybrid Photo Diode (HPD) detectors

Scintillator tile inspection

The CMS HCAL being inserted into the solenoid

CMS Hadron sampling calorimetry

Compensated hadron calorimetry & high precision em calorimetry are incompatible
In CMS, hadron measurement combines HCAL (Brass/scint) and ECAL(PbWO**4**) data
This effectively gives a hadron calorimeter divided in depth into two compartments

Neither compartment is 'compensating': *e/h ~ 1.6* for ECAL and *e/h ~ 1.4* for HCAL
Hadron energy resolution is degraded and response is energy-dependent

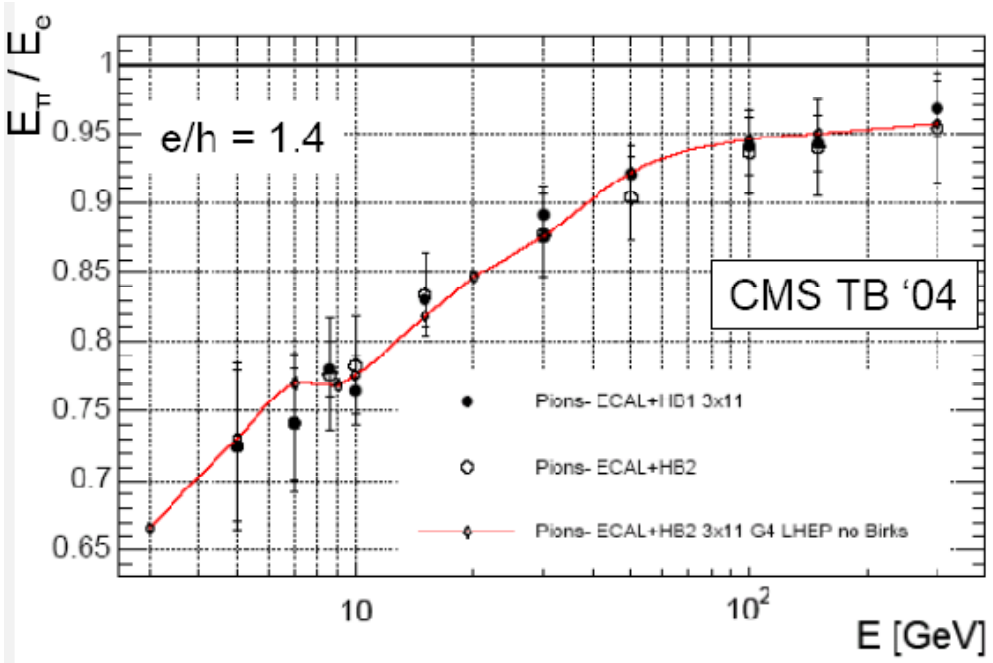

(ECAL+HCAL) raw response to pions vs energy
(red line is MC simulation)

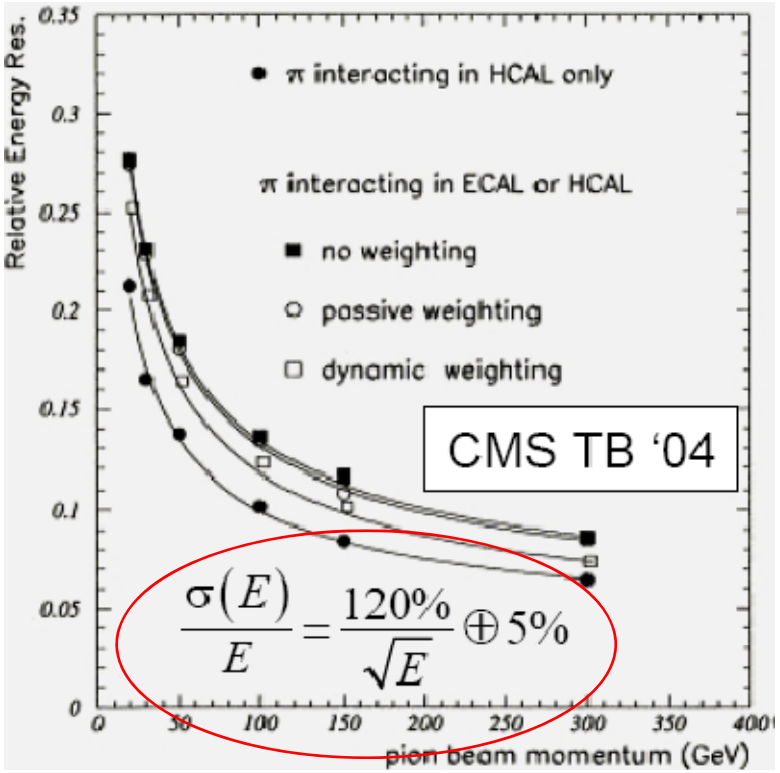

CMS - First data at LHC in 2008

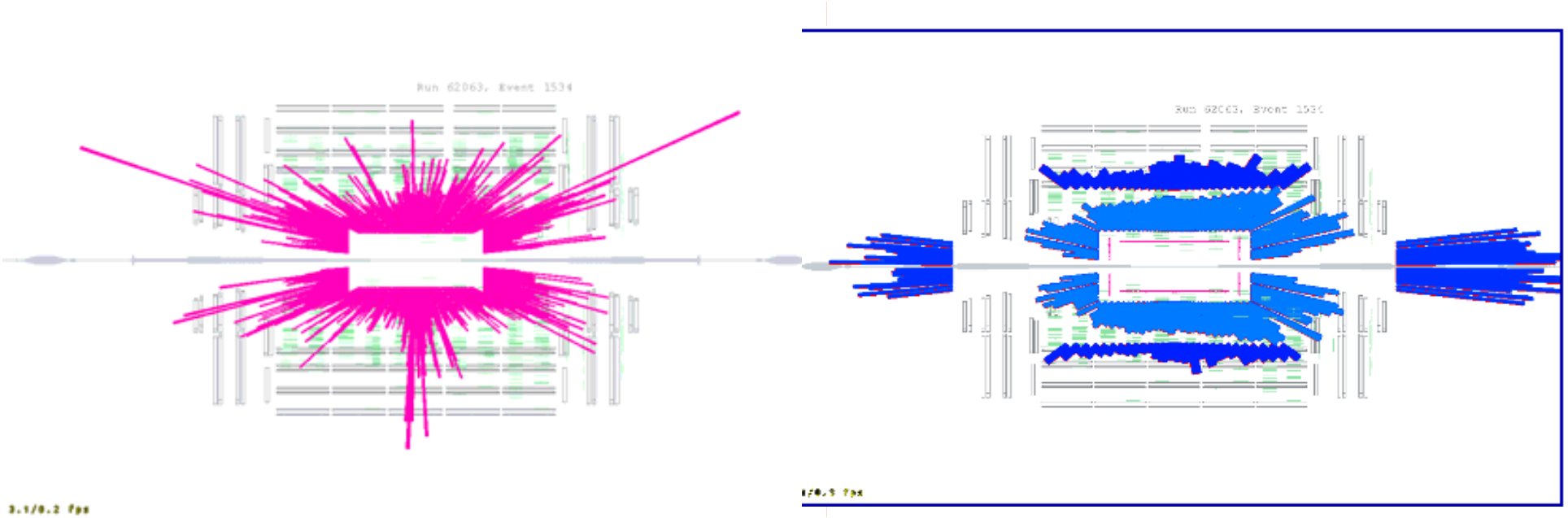

Full crystal ECAL response to an LHC beam ‘splash’ event

Hadron calorimetry response to an LHC beam ‘splash’ event

Summary

- Calorimeters are key elements in almost all particle physics experiments
- They will play a crucial role in discovery physics at the LHC
- A wide variety of mature and new technologies are available
- Calorimeter design is dictated by physics goals and experimental opportunities and constraints
- Compromises often necessary, ie choosing between high resolution e.m. calorimetry or high resolution hadron calorimetry

Special thanks to
Prof RM Brown (RAL, STFC)
C Joram (CERN)
M Diemoz (Roma, INFN)

Ref:
Calorimetry for particle physics, Fabian and Gianotti, Rev Mod Phys, 75, 1243 (2003)
Calorimetry, Energy measurement in particle physics, Wigmans, OUP (200)

Backups

EM showers: transverse profile

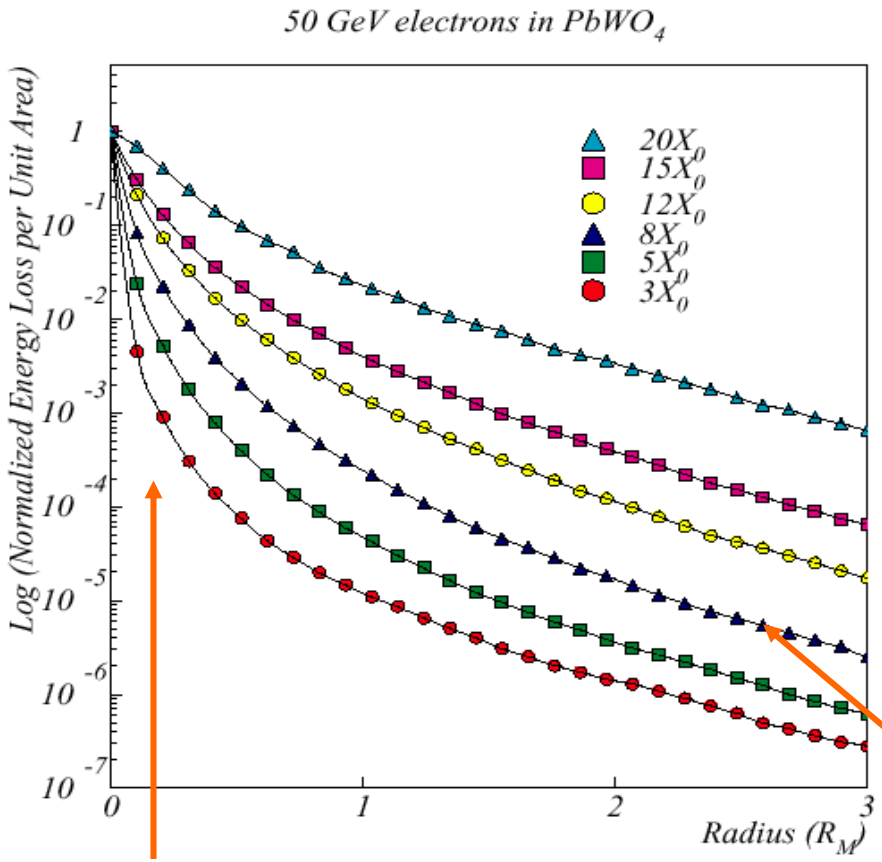

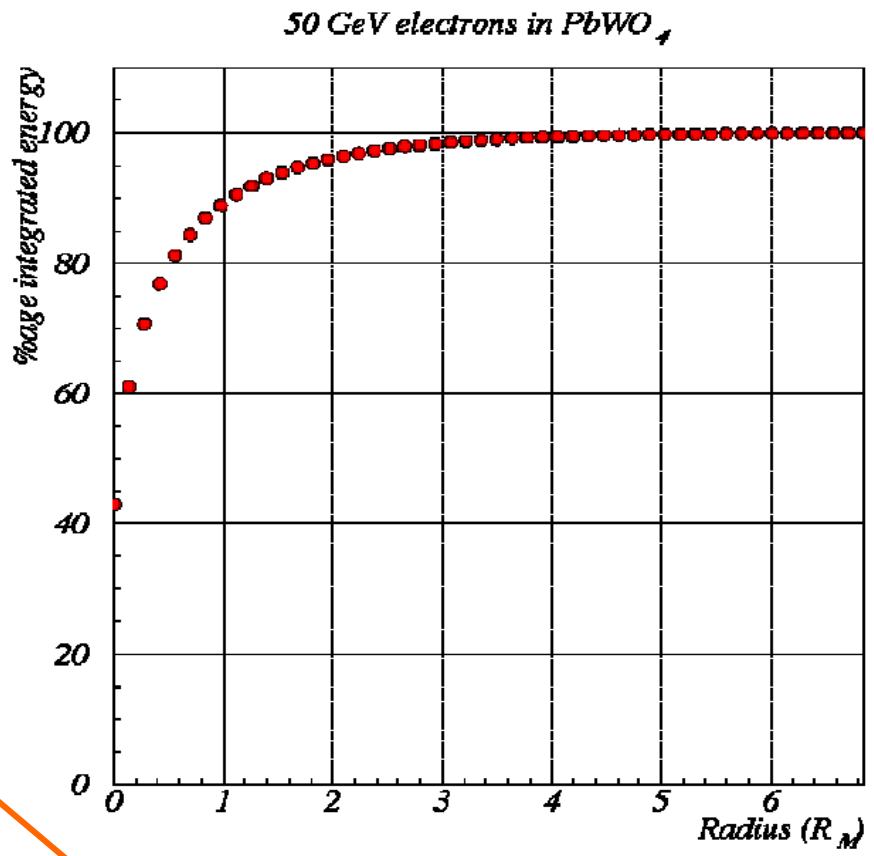

Central core: multiple scattering

Peripheral halo: propagation of less attenuated photons, widens with depth of of the shower

EM showers, logitudinal profile

Shower parametrization

$$\frac{dE}{dt} \propto t^{\alpha} e^{\beta t}$$

Material	Z	A	ρ [g/cm^3]	X_0 [g/cm^2]	λ_a [g/cm^2]
Hydrogen (gas)	1	1.01	0.0899 (g/l)	63	50.8
Helium (gas)	2	4.00	0.1786 (g/l)	94	65.1
Beryllium	4	9.01	1.848	65.19	75.2
Carbon	6	12.01	2.265	43	86.3
Nitrogen (gas)	7	14.01	1.25 (g/l)	38	87.8
Oxygen (gas)	8	16.00	1.428 (g/l)	34	91.0
Aluminium	13	26.98	2.7	24	106.4
Silicon	14	28.09	2.33	22	106.0
Iron	26	55.85	7.87	13.9	131.9
Copper	29	63.55	8.96	12.9	134.9
Tungsten	74	183.85	19.3	6.8	185.0

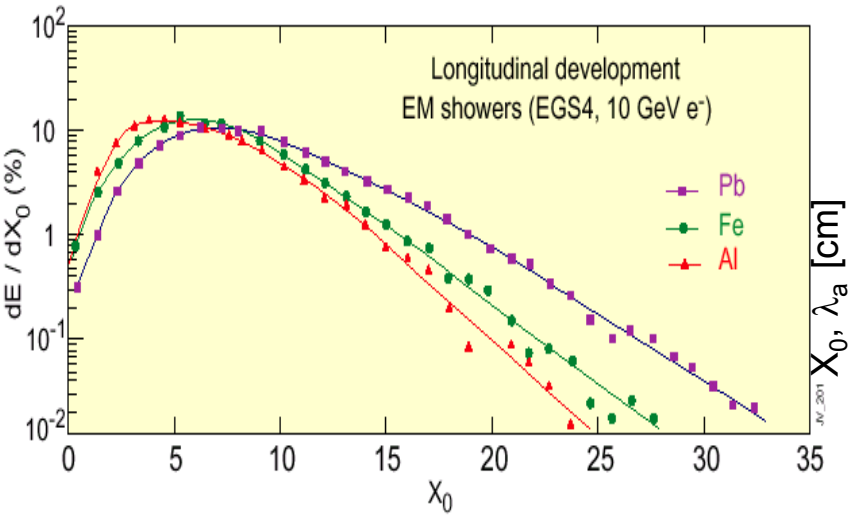

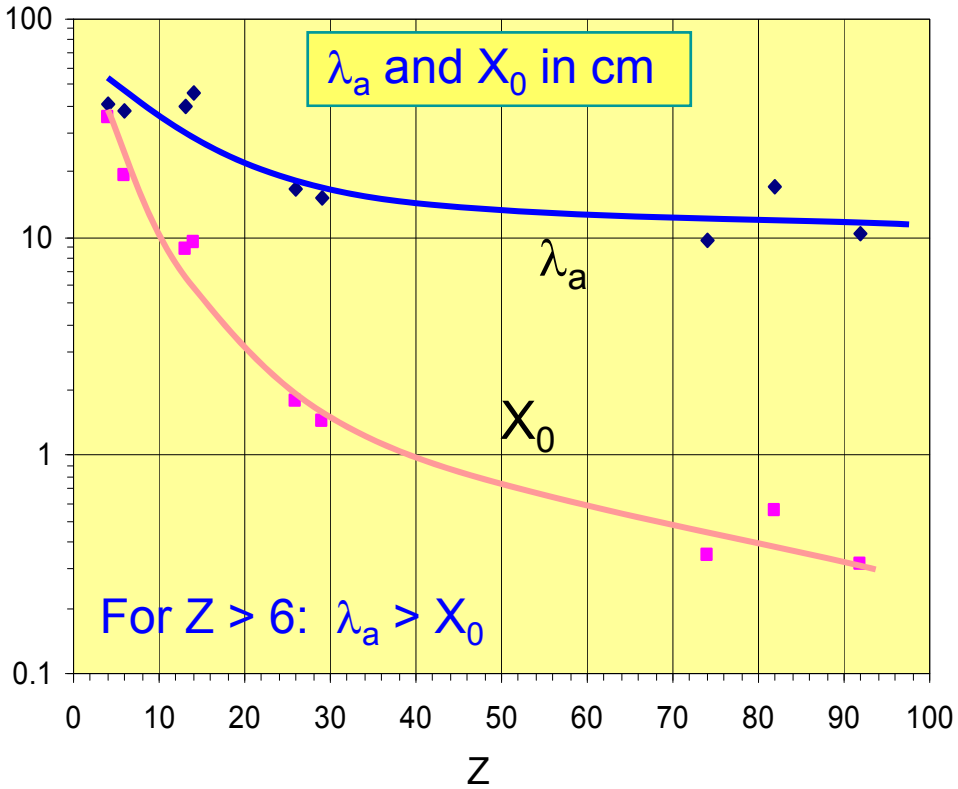

Crystals: building blocks

These crystals make light!

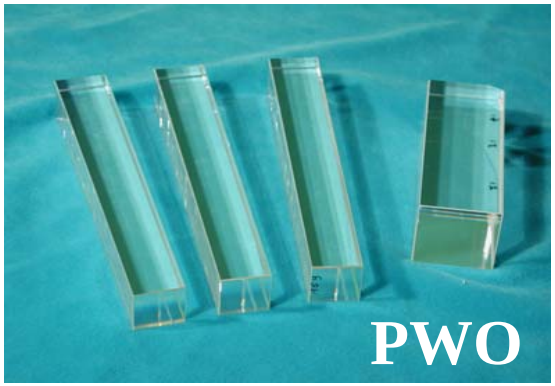

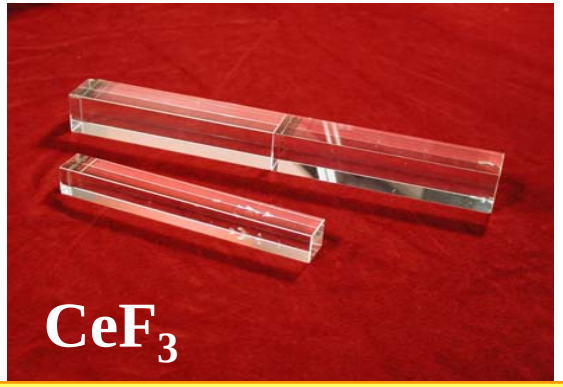

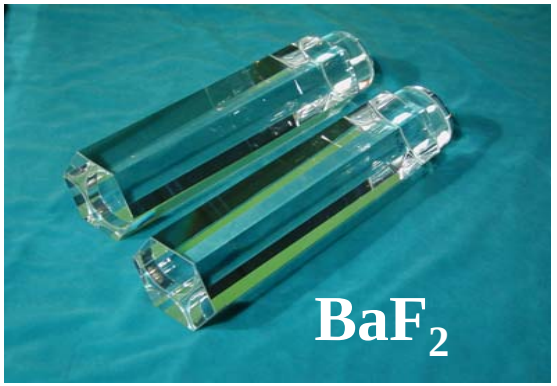

Crystals are basic components of electromagnetic calorimeters aiming at precision

Scintillation: a three step process

Scintillator + Photo Detector = Detector

PMT,PD,APD

How does it works

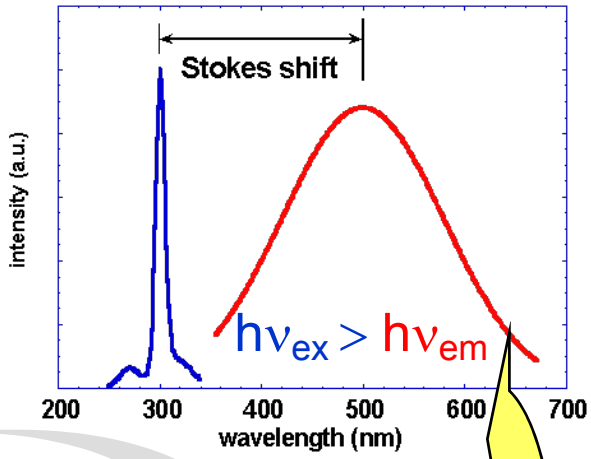

absorption e.g. γ

conversion

emission

$I(E) = I_0(E)e^{-\mu d}$

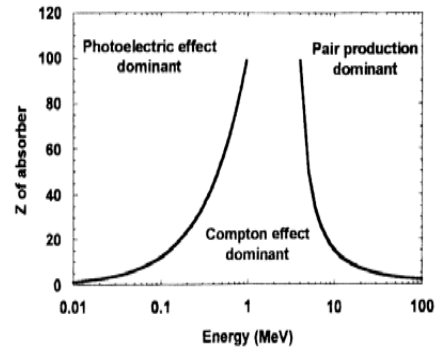

Energy → Excitation

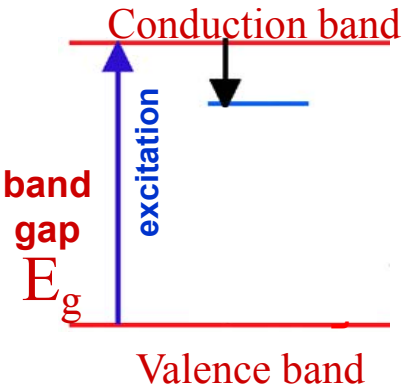

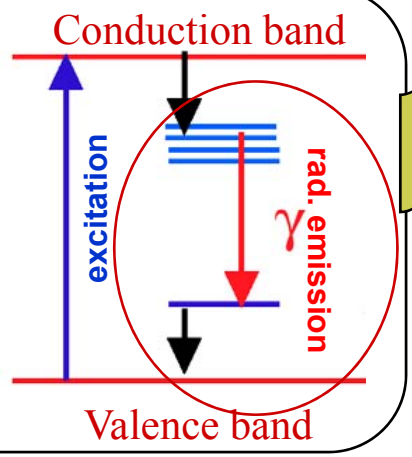

Crystals growing technology

Czochralski method

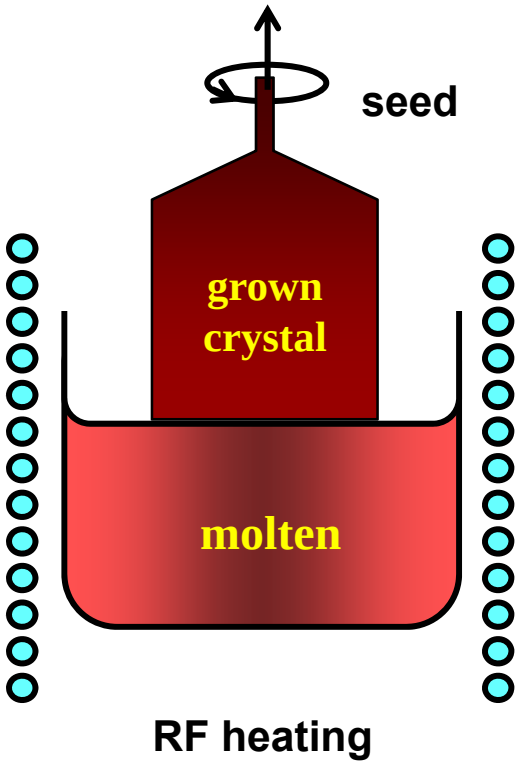

Optimization and equalization of crystals properties may take few years of efforts

Scintillating crystals

Variation in the lattice
(e.g. defects and impurities)
↓
local electronic energy levels in the energy gap

If these levels are unoccupied electrons moving in the conduction band may enter these centres

The centres are of three main types:

- Luminescence centres in which the transition to the ground state is accompaigned by photon emission
- Quenching centres in which radiationless thermal dissipation of excitation energy may occur
- Traps which have metastable levels from which the electrons may subsequently return to the conduction band by acquiring thermal energy from the lattice vibrations or fall to the valence band by a radiationless transition

Scintillating crystals

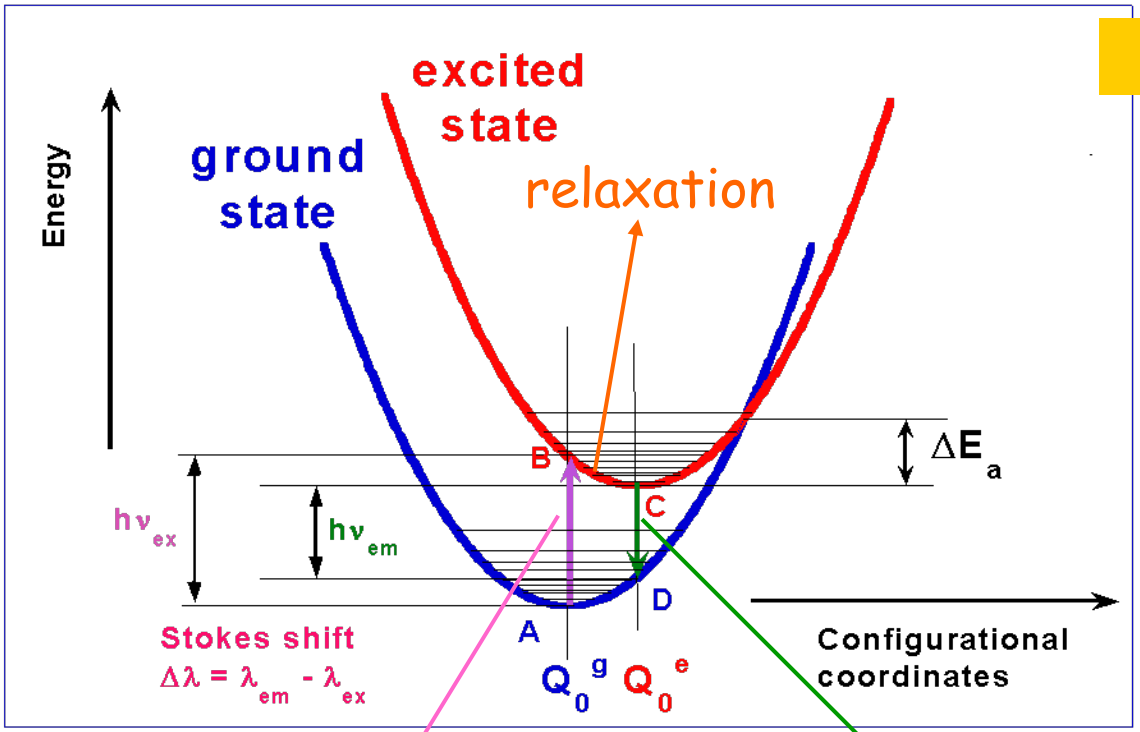

$PbWO_4$: λ_{excit}=300nm ; λ_{emiss}=500nm

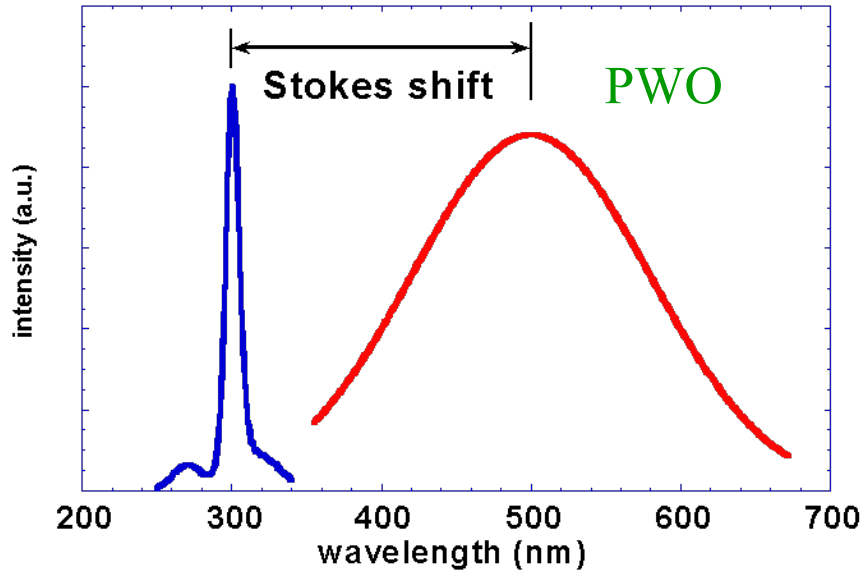

Scintillating crystals

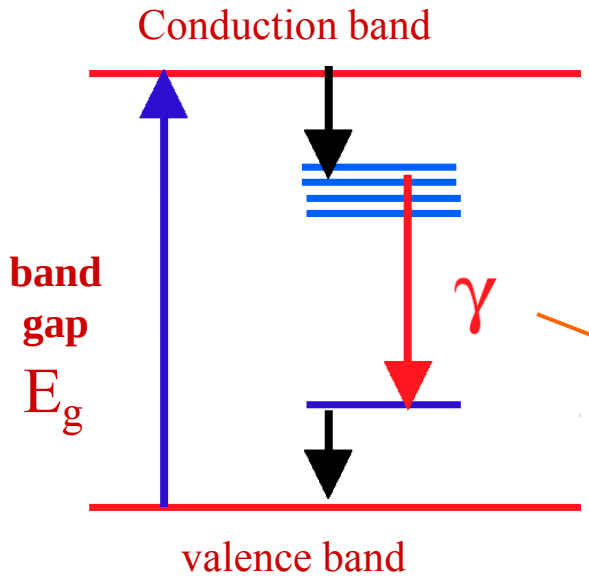

$E_{dep} \rightarrow$ e-h

$E_s = \beta E_g \quad \beta > 1$

$N_{eh} = E_{dep} / \beta E_g$

$N_\gamma = SQN_{eh}$

Efficiency of transfer to luminescent centres

radiative efficiency of luminescent centres

$$\eta_\gamma = N_\gamma / E_{dep} = SQN_{eh} / E_{dep} = \mathbf{SQ/ \beta E_g}$$

- S, Q ≈ 1 , βE_g as small as possible
- medium transparent to λ_{emiss}

Electromagnetic shower

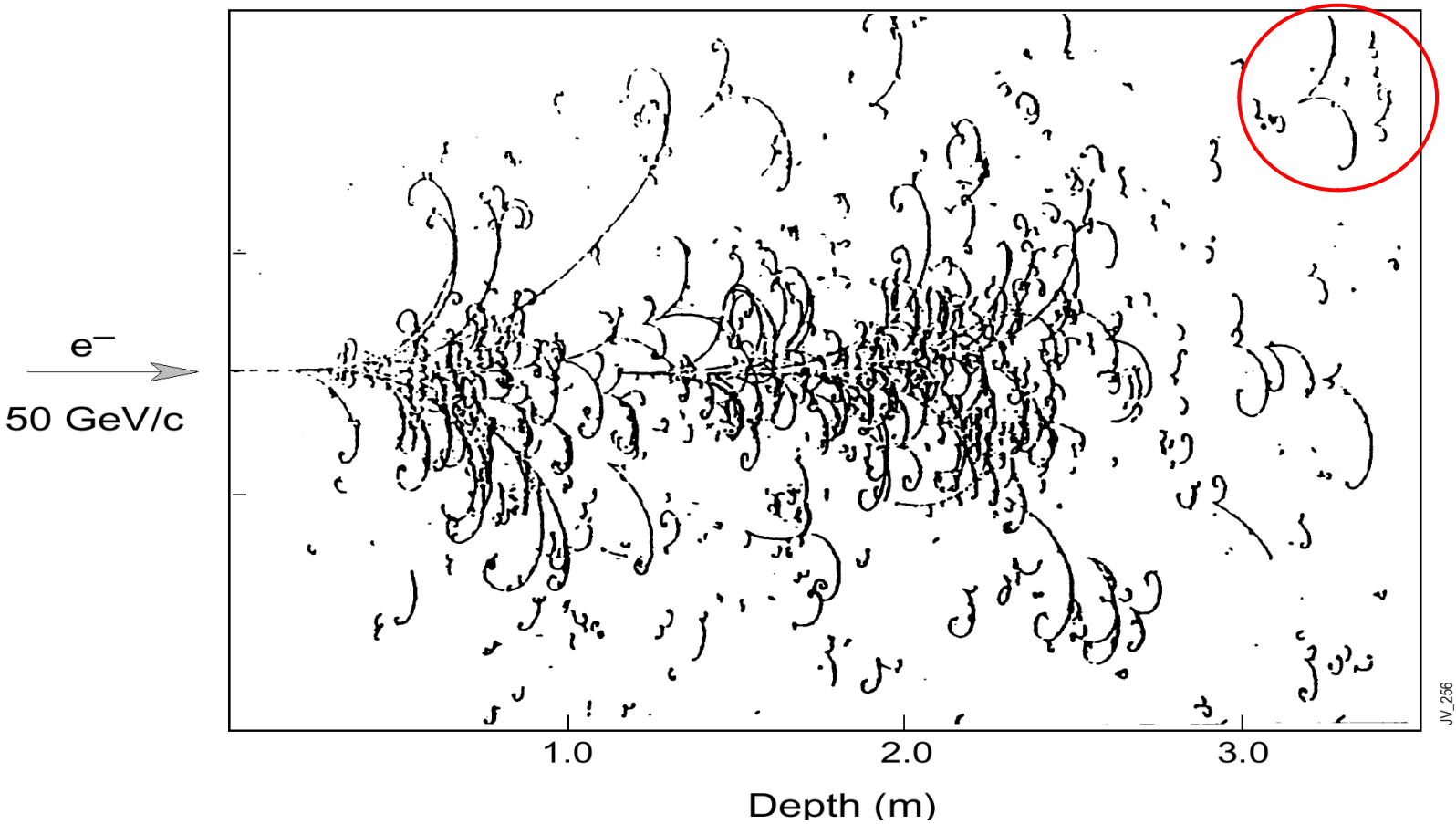

Big European Bubble Chamber filled with Ne:H_2 = 70%:30%,
3T Field, L=3.5 m, $X_0 \approx 34$ cm, 50 GeV incident electron

CMS Barrel and Endcap Homogeneous ECAL

A CMS Supermodule with 1700 tungstate crystals

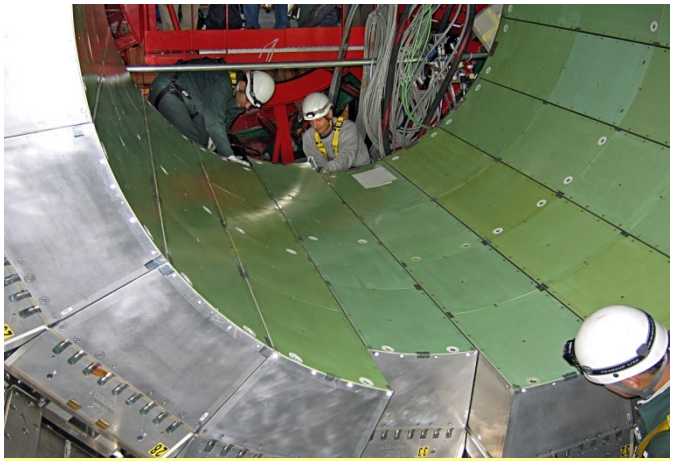

Installation of the last SM into the first half of the barrel

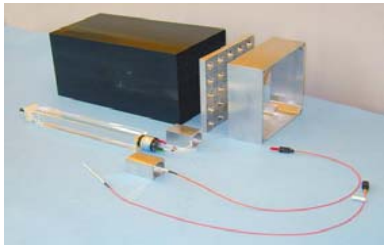

A CMS endcap 'supercrystal' 25 crystals/VPTs

CMS HCAL

Copper has been selected as the absorber material because of its density. The HB is constructed of two half-barrels each of 4.3 meter length. The HE consists of two large structures, situated at each end of the barrel detector and within the region of high magnetic field. Because the barrel HCAL inside the coil is not sufficiently thick to contain all the energy of high energy showers, additional scintillation layers (HOB) are placed just outside the magnet coil. The full depth of the combined HB and HOB detectors is approximately 11 absorption lengths.

The hadron barrel (HB) and hadron endcap (HE) calorimetesr are sampling calorimeters with 50 mm thick copper absorber plates which are interleaved with 4 mm thick scintillator sheets.

CMS HCAL – fibre readout

Megatiles are large sheets of plastic scintillator which are subdivided into component scintillator tiles, of size Δη x Δφ = 0.87 x 0.87 to provide for reconstruction of hadronic showers. Scintillation signals from the megatiles are detected using waveshifting fibers. The fiber diameter is just under 1 mm.

Light emission from the tiles is in the blueviolet, with wavelength in the range λ = 410-425 nm. This light is absorbed by the waveshifting fibers which fluoresce in the green at λ = 490 nm. The green, waveshifted light is conveyed via clear fiber waveguides to connectors at the ends of the megatiles.